The lysophosphatidic acid receptor LPA$_1$ promotes epithelial cell apoptosis following lung injury

Manuela Funke,[1,2] Zhenwen Xhao,[3] Yan Xu,[3] Jerold Chun,[4] and Andrew M. Tager[1,2]

[1]Pulmonary and Critical Care Unit and [2]Center for Immunology and Inflammatory Diseases, Massachusetts General Hospital, Harvard Medical School, Boston, MA 02114, [3]Department of Obstetrics and Gynecology, Indiana University School of Medicine, Indianapolis, Indiana 46202 and [4]Department of Molecular Biology, Dorris Neuroscience Center, The Scripps Research Institute, La Jolla, CA 92037

Address correspondence to:
Andrew M. Tager, M.D.
Pulmonary and Critical Care Unit
Center for Immunology and Inflammatory Diseases
Massachusetts General Hospital
149 13th Street, Room 8301
Charlestown, MA 02129
Email: amtager@partners.org
Voice: (617) 724-7368
Fax: (617) 726-5651

Running Title: LPA$_1$ promotes epithelial cell apoptosis

"This article has an online data supplement, which is accessible from this issue's table of content online at www.atsjournals.org"

1

ABSTRACT

Increased epithelial cell apoptosis in response to lung injury has been implicated in the development of idiopathic pulmonary fibrosis (IPF), but the molecular pathways promoting epithelial cell apoptosis in this disease have yet to be fully identified. Lysophosphatidic acid (LPA), which we have previously demonstrated mediates bleomycin lung injury-induced fibroblast recruitment and vascular leak in mice and fibroblast recruitment in IPF patients, is an important regulator of survival and apoptosis in many cell types. We now show that LPA signaling through its receptor LPA$_1$ promotes epithelial cell apoptosis induced by bleomycin injury. The number of apoptotic cells present in both the alveolar and bronchial epithelia of LPA$_1$-deficient mice was significantly reduced compared to wild type mice at day 3 post-bleomycin challenge, as was lung caspase-3 activity. Consistent with these *in vivo* results, we found that LPA signaling through LPA$_1$ induced apoptosis in normal human-bronchial epithelial cells in culture. LPA-LPA$_1$ signaling appeared to specifically mediate anoikis, the apoptosis of anchorage-dependent cells induced by their detachment. Similarly, LPA negatively regulated attachment of R3/1 rat alveolar epithelial cell line cells. In contrast, LPA signaling through LPA$_1$ promoted the resistance of lung fibroblasts to apoptosis, which has also been implicated in IPF. The ability of LPA-LPA$_1$ signaling to promote both epithelial cell apoptosis and fibroblast resistance to apoptosis may therefore contribute to the capacity of this signaling pathway to regulate the development of pulmonary fibrosis following lung injury.

Keywords: Pulmonary fibrosis; apoptosis; epithelial cells, lysophosphatidic acid; LPA$_1$

INTRODUCTION

Repetitive lung injury and aberrant wound-healing responses are thought to contribute to the pathogenesis of idiopathic pulmonary fibrosis (IPF) (1). We have recently generated evidence that the bioactive lipid lysophosphatidic acid (LPA) may drive several of the wound-healing responses thought to contribute to the development of pulmonary fibrosis following lung injury, including fibroblast recruitment and vascular leak (2). LPA signals through specific G protein-coupled receptors (GPCRs), at least five of which have been definitively established and designated LPA$_1$ to LPA$_5$ (3). We found that mice deficient for one of these receptors, LPA$_1$, are dramatically protected from fibrosis and mortality induced by bleomycin challenge (2). Both fibroblast recruitment and vascular leak were significantly attenuated in LPA$_1$-deficient (LPA$_1$ KO) mice in this model of pulmonary fibrosis. We also found that LPA levels were increased in bronchoalveolar lavage samples from patients with IPF, that LPA$_1$ was highly expressed by fibroblasts recovered from these samples, and that inhibition of LPA$_1$ markedly reduced fibroblast responses to the chemotactic activity of these samples; all suggesting that LPA signaling through LPA$_1$ contributes to the excessive accumulation of fibroblasts that occurs in the lungs of IPF patients.

In addition to mediating fibroblast recruitment and vascular leak, LPA regulates an extensive array of developmental, physiological and pathophysiological processes, including cell proliferation, differentiation, cytoskeletal rearrangement, and survival. With respect to cell survival, LPA has pervasive but varied effects, promoting either the survival or apoptosis of many different cell types (4). Exaggerated lung epithelial cell apoptosis appears to play a central role in pulmonary fibrogenesis. Increased numbers of apoptotic cells have been observed in both the alveolar and bronchial epithelia of IPF patients (5, 6). Induction of pulmonary epithelial cell

apoptosis in mice, either by pulmonary delivery of anti-Fas antibody (7, 8) or transgenic

overexpression of transforming growth factor (TGF-β) (9), results in the development of fibrosis,

as does targeted injury of alveolar epithelial cells (10). Epithelial cell apoptosis is also

prominent in the bleomycin model of pulmonary fibrosis, in which intratracheal challenge leads

to the rapid appearance of apoptosis in bronchial and alveolar epithelial cells. This early phase

of apoptosis resolves, but is followed by a second wave of apoptosis in the second week post-

challenge (11). To investigate whether LPA contributes to increased epithelial cell apoptosis

induced by fibrogenic lung injury, we compared the time course of apoptosis induced by

intratracheal bleomycin challenge in wild type (WT) and LPA$_1$-deficient (LPA$_1$ KO) mice. We

found that the early phase of apoptosis was significantly attenuated in the absence of LPA$_1$

expression, suggesting that LPA signaling through LPA$_1$ promotes epithelial cell apoptosis.

Consistent with these *in vivo* results, we found that LPA signaling through LPA$_1$ induced

apoptosis in normal bronchial airway epithelial (NHBE) cells in culture.

In contrast, LPA signaling through the same receptor, LPA$_1$, promoted resistance of

primary mouse lung fibroblasts (PMLF) to apoptosis. Fibroblasts and myofibroblasts appear to

be abnormally resistant to apoptosis in IPF (12). In addition to the abilities of LPA and LPA$_1$ to

promote fibroblast recruitment and vascular leak, LPA-LPA$_1$ signaling therefore may also

contribute to the development of pulmonary fibrosis following lung injury by promoting

epithelial cell apoptosis but fibroblast resistance to apoptosis. Loss of these effects of LPA-

LPA$_1$ signaling on epithelial cell and fibroblast apoptosis may therefore represent two additional

mechanisms through which LPA$_1$ KO mice are dramatically protected from bleomycin-induced

fibrosis, as we have previously observed (2). Some of the data presented in this paper have

previously been reported in abstract form (13).

4

MATERIAL AND METHODS

Animals and bleomycin administration

Experiments comparing LPA$_1$ KO and wild type (WT) mice used sex- and weight-matched

offspring of mice heterozygous for the LPA$_1$ mutant allele, which were hybrids of the C57Bl/6

and 129Sv/J genetic backgrounds (14). These mice consequently on average had similar

assortments of genes from the C57Bl/6 and 129Sv/J backgrounds. Experiments measuring BAL

LPA concentrations used WT C57Bl/6 mice purchased from NCI-Frederick Mouse Repository.

All bleomycin-challenged mice received 3U/kg of bleomycin (Gensia Sicor Pharmaceuticals,

Irvine, CA, USA) in a total volume of 50µl sterile saline by intratracheal injection. All

experiments used mice that were 6 to 10 weeks of age, and all mice were maintained in a specific

pathogen–free (SPF) environment certified by the American Association for Accreditation of

Laboratory Animal Care (AAALAC). All experiments were performed in accordance with

National Institute of Health guidelines and protocols approved by the Massachusetts General

Hospital Subcommittee on Research Animal Care.

Lung immunohistochemical and immunofluorescence staining

Lungs excised for immunostaining were inflated to 25 cm H$_2$O and fixed with 10% buffered

formalin. Terminal deoxynucleotidyl transferase dUTP nick end labeling (TUNEL)$^+$, p53$^+$ and

p21$^+$ cells, and TUNEL$^+$/T1α^+ and TUNEL$^+$/pro-surfactant protein C$^+$ cells were identified in

multiple paraffin-embedded 5µm sections of the entire mouse lung by immunohistochemical and

immunofluorescence staining as described in the additional methods section of the Online Data

Supplement.

Lung caspase-3 activity

Caspase-3 activity was determined in homogenates of whole sets of mouse lungs using a Caspase-3 Fluorometric Assay Kit (Biovision, Mountain View, CA, USA) according to the manufacturer's instructions.

Mouse bronchoalveolar lavage and LPA analysis

BAL samples for analysis of LPA levels were obtained as previously described (2). LPA concentrations were determined by electrospray ionization mass spectrometry (ESI-MS) by an investigator blinded to the identity of the samples, also as previously described (15). Concentrations of 16:0, 18:0, 18:1, 18:2, 20:4 and 22:6 LPA were measured, and added to determine total BAL LPA concentrations.

NHBE, R3/1 and PMLF cell culture, and apoptosis, detachment and attachment assays

Normal human bronchial epithelial (NHBE) cells (Lonza, Basel, Switzerland) were initially cultured in tissue culture-treated polystyrene flasks (Corning, Lowell, MA, USA) in bronchial epithelial cell growth medium (BEGM®, Lonza) according to the manufacturer's instructions, and used when 60 to 70% confluent at passages 5 to 8. R3/1 cells, a rat alveolar epithelial cell line with several characteristic features of type I cells (16, 17), were the kind gift of Dr. Roland Koslowski (University of Technology, Dresden, Germany) and were cultured in DMEM medium with 10% FBS (DMEM-10%). Primary mouse lung fibroblasts (PMLF) were isolated from WT and LPA_1 KO mice and cultured in TC-treated polystyrene flasks in DMEM with 15% FBS (DMEM-15%) according to the standard methods of our laboratory (18). All cells were cultured

at 37°C and 5% CO$_2$ in a humidified incubator. NHBE cells and PMLF apoptosis assays, and

NHBE cells and R3/1 cell detachment and attachment assays, were performed as described in the

Online Data Supplement.

NHBE cell cytofluorescence staining

NHBE cells for fluorescence staining were transferred to Lab-Tek™ 4 well Permanox™

chamber slides (Nunc-Nalgene, Thermo Scientific, Rochester, NY, USA) at 50,000 cells/well,

and cultured directly in BEGM with 0.1% fatty acid-free BSA (FAF-BSA, Sigma Aldrich, St.

Louis, MO, USA) with or without 18:1 LPA (Avanti Polar Lipids, Alabaster, AL, USA) for 3h.

Cells were fixed with paraformaldehyde, and labeling of vinculin or F-actin was then performed

with fluorescein isothiocyanate (FITC)-conjugated mouse anti-human vinculin antibody (Sigma

Aldrich) or fluorescein phalloidin (Molecular Probes, Invitrogen), respectively. Slides were then

mounted with VECTASHIELD® mounting medium with DAPI (Vector Laboratories).

Statistics

Differences between groups in experiments with two groups were analyzed for statistical

significance with two-tailed Student's T-tests, using Microsoft Excel software. Differences

between groups in experiments with more than two groups were analyzed for statistical

significance by one-way ANOVA. When ANOVA rejected the hypothesis of equality of the

group means, pairwise comparisons were made between groups with Bonferroni post-test

corrections. *P*-values of < 0.05 were considered statistically significant for all comparisons, and

all errors represent SEM.

RESULTS

Bleomycin-induced apoptosis of the alveolar epithelium is dependent on LPA_1.

Bleomycin delivered as a single intratracheal challenge has been demonstrated to lead to the rapid appearance of apoptosis in both bronchial and alveolar epithelial cells. This early phase of apoptosis resolves, but is followed by another wave of apoptosis in the second week post-challenge (11). To determine if LPA-LPA_1 signaling influenced epithelial cell apoptosis during the development of pulmonary fibrosis, we first compared the time course of alveolar epithelial apoptosis induced by bleomycin in the lung parenchyma of WT and LPA_1 KO mice. TUNEL staining of lung sections from mice sacrificed at multiple time points following bleomycin challenge demonstrated that the early phase of apoptosis was significantly attenuated in the absence of LPA_1 expression (Figure 1A - C). Minimal numbers of TUNEL$^+$ cells were present in the lungs of both WT and LPA_1 KO mice at baseline on day 0, prior to bleomycin challenge (Supplemental Figure E1A, B). The number of TUNEL$^+$ cells increased in the alveolar epithelium of WT mice at day 1 after bleomycin challenge, remained elevated at day 3, and declined at day 5 (Figure 1A, C). The number of TUNEL$^+$ cells in the alveolar epithelium of LPA_1 KO mice increased to levels similar to those of WT mice at day 1 post-bleomycin, but declined earlier. Consequently at day 3 post-challenge, TUNEL$^+$ cells were reduced by 67% in LPA_1 KO compared to WT mice (Figure 1B, C).

To confirm that the early phase of bleomycin-induced apoptosis was attenuated in the lung in absence of LPA_1 expression, we compared the expression of p53 and p21, and the activity of caspase 3, in WT and LPA_1 KO mice at day 3 post-bleomycin. Upregulation of the tumor suppressor/apoptosis regulatory proteins p53 and p21 has been demonstrated in apoptotic cells in both the alveolar and bronchial epithelia of patients with IPF (5, 6), and in mouse

alveolar epithelial cells during the early phase of bleomycin-induced apoptosis (19). Minimal numbers of $p53^+$ and $p21^+$ cells were present in the lungs of both WT and LPA_1 KO mice at day 0 (Supplemental Figure E1C – F). The increase in the number of $p53^+$ cells observed at day 3 following bleomycin challenge was significantly attenuated in the lungs of LPA_1 KO compared with WT mice (Figure 1D – F); at this time point, $p53^+$ cells were reduced by 84% in LPA_1 KO compared to WT mice. The increase in the number of $p21^+$ cells at day 3 post-bleomycin was similarly attenuated in LPA_1 KO mice (Figure 1G – I), with 74% fewer $p21^+$ cells being present in LPA_1 KO compared with WT mice. Upregulation of caspase 3, one of the effector caspases of apoptosis, has also been associated with apoptosis of bronchiolar and alveolar epithelial cells both in IPF patients (6) and bleomycin-challenged mice (20). The increase in lung caspase 3 activity induced by bleomycin at day 3 post-challenge was significantly mitigated in LPA_1 KO mice (Figure 1J); at this time point, lungs from LPA_1 KO mice contained 55% less caspase 3 activity compared with WT lungs. At day 1 post-challenge, lung caspase 3 activity was increased to a similar extent in LPA_1 KO and WT mice, although the increases were not significant in either genotype (data not shown).

To determine whether apoptotic cells in the alveolar epithelium of WT and LPA_1 KO mice at early time points post-bleomycin challenge were type I or type II alveolar epithelial cells (AECs), we performed TUNEL staining in conjunction with immunohistochemical staining of either T1α, a marker of type I AECs (21) (Supplemental Figure E2), or pro-surfactant protein C (proSP-C), a marker of type II AECs (Supplemental Figure E3), on lung sections from mice sacrificed either at day 0 pre-bleomycin challenge or at day 3 post-bleomycin. As seen previously, minimal numbers of $TUNEL^+$ cells were present in the lungs of both WT and LPA_1 KO mice at baseline on day 0 (Supplemental Figures E2A and B and E3A and B). At day 3

post-bleomycin challenge, most TUNEL^{+} cells in both WT and LPA_1 KO mice demonstrated co-staining for T1α, (Supplemental Figure E2C and D). The specificity of T1α staining for Type I AECs is demonstrated in Supplemental Figure E2E, in which T1α expression is absent from the pulmonary endothelium, the bronchial epithelium, and cells in the alveolar epithelium that appear to be type II AECs. In contrast, few TUNEL^{+} cells in both genotypes of mice demonstrated co-staining for the type II AEC marker pro-SPC at day 3 post-challenge (Supplemental Figure E3C and D). However, whereas proSP-C staining appeared uniform throughout the lung parenchyma at day 0 pre-bleomycin, staining for this type II cell marker appeared to decrease in areas of lung injury at day 3 post-challenge. As shown in Supplementary Figure E3E, there was a paucity of pro-SPC staining in areas with substantial numbers of TUNEL^{+} cells, consistent with a prior report of type II cell expression of SPC declining following bleomycin challenge (22). Therefore, although our staining suggests that substantial apoptosis of type I AECs occurs at day 3 post-bleomycin challenge, we cannot exclude the possibility that substantial type II cell apoptosis is concurrently occurring.

Bleomycin-induced apoptosis of the bronchial epithelium is dependent on LPA_1.

As noted, increased numbers of apoptotic cells have been observed in the bronchial epithelium as well as in the alveolar epithelium in both the bleomycin model of pulmonary fibrosis (11), and in the lungs of IPF patients (5, 6). We therefore also compared the time course of bronchial epithelial apoptosis induced by bleomycin in the airways of WT and LPA_1 KO mice. TUNEL staining of lung sections from mice sacrificed at multiple time points following bleomycin challenge demonstrated that the early phase of apoptosis was also significantly attenuated in the bronchial epithelium in the absence of LPA_1 expression (Figure 2A - G). No

TUNEL$^+$ cells were observed in the airways of either WT or LPA_1 KO mice at baseline on day 0,

prior to bleomycin challenge (Figure 2A, B and G). As observed in the alveolar epithelium, the

number of TUNEL$^+$ cells increased in the bronchial epithelium of WT and LPA_1 KO mice to a

similar extent at day 1 after challenge (Figure 2C, D and G). However, as also observed in the

alveoli, the number of TUNEL$^+$ cells in the airways of LPA_1 KO mice declined earlier than in

WT mice, so that at day 3 post-challenge, TUNEL$^+$ cells were reduced by 76% in LPA_1 KO

compared to WT mice (Figure 2E, F and G). Taken together, our results indicate that apoptosis

induced early after bleomycin injury is significantly reduced in both the airways and the alveoli

in the absence of LPA-LPA_1 signaling in LPA_1 KO mice.

LPA accumulates in the airspaces early after bleomycin lung injury.

We have previously reported that LPA is present in increased concentrations in BAL

recovered from mice at later time points post-bleomycin challenge, from day 5 to day 14,

indicating that it accumulates in the airspaces at these times (2). The dependence of bronchial

and alveolar epithelial apoptosis on LPA_1 expression earlier after bleomycin suggests that

increased amounts of LPA are also present in the lungs prior to these time points. To confirm

this, we measured the concentrations of six major LPA species (16:0, 18:0, 18:1, 18:2, 20:4 and

22:6 LPA) in BAL recovered from unchallenged mice (day 0) and mice 1 and 3 days post-

bleomycin challenge by electrospray ionization mass spectrometry (ESI-MS). Of these six LPA

species, 16:0 and 22:6 are the most abundant in the plasma of unchallenged mice (23). The BAL

concentrations of each of these species except 22:6 LPA increased at these early time points

(Figure 3A). 18:0 LPA demonstrated the greatest increase, rising 3.5-fold between days 0 and 1,

and then returning to its baseline level at day 3. Total BAL LPA concentrations, determined as

the sum of the six major species of LPA measured, were elevated at both 1 and 3 days post-bleomycin challenge (Figure 3B). Increased levels of LPA were therefore present in the airspaces early post-bleomycin challenge, when bronchial and alveolar epithelial apoptosis was found to depend on LPA_1 expression. Although we have not formally evaluated BAL levels of LPA in bleomycin-challenged LPA_1 KO mice, we have previously found evidence to suggest that the generation of LPA is preserved in these mice deficient for one of LPA's receptors (2).

LPA induces epithelial cell apoptosis through its receptor LPA_1.

To investigate whether LPA is able to induce lung epithelial cell apoptosis by acting directly on these cells, we determined the effects of LPA on normal human bronchial epithelial (NHBE) cell apoptosis in culture. Apoptotic cells were identified in these experiments by flow cytometry following staining with annexin V and propidium iodide (24), as annexin V-positive, PI-negative cells (Supplemental Figure E4). The effects of mediators on lung epithelial cell apoptosis have been demonstrated to depend on the extracellular matrix proteins with which the cells are in contact. For example, TGF-β has been demonstrated to induce apoptosis of lung epithelial cells grown on matrigel, which is representative of basement membrane proteins normally present in the lung, but not of lung epithelial cells grown on fibronectin, which is representative of the extracellular matrix present in the injured or fibrotic lung (25). To investigate the effects of LPA on epithelial cell apoptosis early after lung injury prior to significant matrix remodeling, we exposed subconfluent NHBE cells grown on matrigel to 1μM LPA. This concentration of LPA significantly induced NHBE cells apoptosis (Figure 4A). We have previously found that the process of collecting BAL dilutes the mouse epithelial lining fluid approximately 65-fold (18). Accounting for this dilution, our BAL measurements indicate that

LPA concentrations in this range were present in the lungs at days 1 and 3 post-bleomycin challenge. Of note, LPA concentrations are unlikely to be uniform throughout the epithelial lining fluid after bleomycin challenge. Rather, at focal sites of lung injury and repair, LPA epithelial lining fluid concentrations would be expected to be considerably higher than determined by our BAL measurements. These data thus suggest that direct effects of LPA on lung epithelial cells contribute to the epithelial apoptosis observed early after bleomycin injury.

In our experiments with NHBE cells, we found that exposure to LPA made these cells noticeably easier to detach with trypsin-EDTA. To begin to examine whether promotion of NHBE cell detachment might contribute to LPA's ability to induce apoptosis in these cells, we compared the effect of LPA on the apoptosis of subconfluent NHBE cells grown in low versus high attachment conditions. Standard tissue culture polystyrene is treated to make its surface negatively charged and hydrophilic when medium is added, promoting cell attachment and spreading (26). The surface of polystyrene that is not tissue culture treated remains neutrally charged and hydrophobic, reducing cell attachment. In contrast to cells grown on matrigel, which we used to model physiologic basement membrane composition, LPA did not significantly induce apoptosis of NHBE cells grown on high attachment tissue culture-treated polystyrene (data not shown). LPA did significantly and dose-dependently induce apoptosis of NHBE cells grown on low attachment (not tissue culture-treated) polystyrene (Figure 4B), leading us to hypothesize that LPA's ability to promote epithelial cell apoptosis is dependent on its ability to promote epithelial cell detachment, a hypothesis we subsequently explored further.

In the experiments presented in Figures 4A and B, we demonstrated that LPA promotes NHBE apoptosis using 18:1 LPA, the most commonly used laboratory reagent for activation of LPA receptors (3). As presented in Figure 3A however, 18:0 was the LPA species largely

responsible for the increase in BAL LPA concentration observed at day 1 post-bleomycin

challenge. We therefore investigated the effects of 18:0 LPA on NHBE apoptosis as well, and

found that it also significantly induced NHBE apoptosis at a concentration of 1 μM (Figure 4C).

Given this similarity in the effects of 18:0 and 18:1 LPA on NHBE apoptosis, the rest of our

experiments were performed with 18:1 LPA only.

To investigate which of LPA's receptor(s) mediate its ability to induce lung epithelial cells

apoptosis, we first assessed NHBE cell mRNA expression of the five established, high-affinity

cognate receptors LPA$_1$–LPA$_5$, as well as P2Y5, a relatively low-affinity receptor that is likely to

join the LPA receptor family as LPA$_6$ (3). Consistent with previously reported results (27), we

confirmed that these cells predominantly expressed LPA$_1$, LPA$_2$ and LPA$_3$ (Supplemental Figure

E5). To distinguish between these three receptors, we determined whether 18:0 LPA-induced

NHBE cell apoptosis was inhibited by AM095, a new LPA receptor antagonist that we have

recently demonstrated to be highly specific for LPA$_1$ (28). This antagonist has been

demonstrated to inhibit LPA activation of LPA$_1$ in a dose-dependent manner (29). AM095

essentially completely abrogated the ability of 18:0 LPA to induce NHBE cell apoptosis (Figure

4C), suggesting that the pro-apoptotic effects of LPA on NHBE cells were mediated by LPA$_1$.

LPA induces epithelial cell apoptosis through detachment.

The detachment of anchorage-dependent cells such as epithelial cells induces apoptosis, a

phenomenon termed "anoikis" (Greek, meaning the state of being without a home) (30). To

investigate whether LPA induces lung epithelial cell apoptosis through the process of anoikis, we

first confirmed the ability of LPA to induce epithelial cell detachment. We performed

detachment assays in which NHBE cells were transferred to low attachment tissue culture plates,

and then incubated with or without LPA for two hours. The tissue culture plates were then

centrifuged in an inverted position, and the cells remaining in the wells were quantified. The

adherence index of NHBE cells exposed to 1μM LPA was 0.54, i.e. LPA's ability to promote

epithelial cell detachment reduced the cells remaining attached in these assays by 46% (Figure

5A). We also investigated the ability of LPA to inhibit epithelial cell attachment in spreading

assays in which the flattening of adherent cells is used to indicate their adhesion. Without

exposure to LPA, 97% of NHBE cells had attached and flattened by 3 hours after transfer to high

attachment tissue culture-treated polystyrene plates. In contrast, only 40% of NHBE cells

incubated with 1μM LPA had attached and flattened in the same time period (Figure 5B). A

broad range of LPA concentrations was able to inhibit the adhesion of unattached NHBE cells in

these spreading assays, with statistically significant reductions in NHBE spreading produced by

LPA concentrations as low as 0.01μM LPA (Supplemental Figure E6). LPA therefore both

promotes the detachment of adherent NHBE cells, and inhibits the adhesion of unattached NHBE

cells, suggesting that LPA may induce epithelial cell apoptosis following bleomycin lung injury

by inducing anoikis.

In the process of anoikis, cell detachment from the extracellular matrix (ECM) induces

apoptosis by disrupting survival signals generated by cell integrin-ECM interactions (31). These

survival signals are generated through cytoskeletal rearrangements induced by integrin-ECM

interactions, including the formation of focal adhesions (FAs) and actin filament stress fibers

(32, 33). We therefore also investigated the effects of LPA on FA and actin stress fiber

formation in lung epithelial cells. We compared the development of FAs, identified by staining

of the FA structural protein vinculin, in NHBE cells 3 hours after transfer to high attachment

tissue culture-treated permanox slides, in the presence or absence of 1 μM LPA. NHBE cells

seeded in the absence of LPA developed FAs, whereas LPA present at the time cells were transferred essentially completely inhibited initial FA formation (Figure 5C, D). Similarly, actin stress fibers were observed in NHBE cells 3 hours after transfer to tissue culture-treated permanox slides in the absence of LPA, whereas 1 μM LPA present at the time cells were transferred essentially completely inhibited actin stress fiber formation as well (Figure 5E, F).

To determine whether LPA also promotes the apoptosis of lung epithelial cells that have already become detached, we investigated the effects of LPA on NHBE cells cultured on ultra low attachment plastic. This plastic is treated to be neutrally charged and hydrophilic, in order to maintain cells in a suspended, unattached state. The presence or absence of 1 μM LPA did not significantly affect the percentage of NHBE cells that were apoptotic 24 hours after transfer to ultra low attachment plastic (Figure 5G), indicating that LPA did not further increase the apoptosis of NHBE cells that were already unattached. These data further support our hypothesis that LPA's pro-apoptotic effects on lung epithelial cells results from its ability to induce the detachment of these cells.

As noted, increased numbers of apoptotic cells have been observed in both the alveolar and bronchial epithelia of IPF patients (5, 6), and we found that bleomycin-induced apoptosis was reduced in both the alveolar and bronchial epithelia of LPA$_1$ KO mice. To investigate whether LPA also negatively regulates the attachment of alveolar epithelial cells in addition to NHBE cells, we investigated the effect of LPA on the spreading of R3/1 rat alveolar epithelial cell line cells. The R3/1 cell line, derived from fetal rat lung (16), express cytokeratins of the simple epithelial type numbers 7, 8, 18 and 19, which are characteristic for rat alveolar epithelial cells, as well as a variety of proteins typical, though not exclusive, for the type I cell phenotype, such as T1α, ICAM-1, Cav-1 and Cav-2 (17). Additionally, two of the three lectins known to

bind to the surface of type I AECs, BPA (*Bauhinia purpurea* agglutinin) and SBA (soybean

agglutinin) bind to R3/1 cells. R3/1 cells also express moderate levels at the type II cell proteins

for SP-A and SP-B, though not SP-C or SP-D (17). These cells consequently have been

suggested to be a suitable tool for the *in vitro* study of alveolar epithelial cell biology (17),

though they do resemble type I cells more than type II. We first confirmed that R3/1 cells

express the LPA1 receptor (Supplemental Figure E7A). As demonstrated in Figure 5H and

Supplemental Figure E7B and C, without exposure to LPA, 97% of R3/1 cells had attached and

flattened by 3 hours after transfer to high attachment tissue culture-treated polystyrene plates,

whereas only 64% and only 29% of R3/1 cells incubated with 1µM or 20µM LPA respectively

had attached and flattened in the same time period. LPA therefore appears to negatively regulate

the attachment of both alveolar and bronchial epithelial cells, although we have not investigated

primary alveolar epithelial cells.

LPA prevents fibroblast apoptosis through LPA$_1$

We have previously reported that LPA signaling through LPA$_1$ contributes to fibroblast

accumulation in the lung following bleomycin injury by promoting the migration of these cells

(2). In contrast to our findings with lung epithelial cells, LPA has been reported to prevent

apoptosis in NIH 3T3, Swiss 3T3, and Rat-1 fibroblast cell lines (34), although the LPA

receptor(s) mediating these anti-apoptotic effects were not identified. Such anti-apoptotic effects

on fibroblasts could also contribute to LPA-induced fibroblast accumulation following

bleomycin lung injury, and we therefore analyzed the effects of LPA on the apoptosis of primary

mouse lung fibroblasts (PMLF). PMLF apoptosis induced by serum deprivation for 24 hours

was completely prevented by LPA concentrations as low as 1 µM (Figure 6A). Lower LPA

concentrations produced trends toward reduced PMLF apoptosis, but these were non-significant

(Supplemental Figure E8). Of the established LPA receptors LPA$_1$ – LPA$_5$, we previously

reported that PMLF predominantly express LPA$_1$ (2). We consequently hypothesized that LPA's

ability to prevent fibroblast apoptosis is mediated by LPA$_1$, the same receptor that mediates

LPA's ability to promote epithelial cell apoptosis. To investigate this hypothesis, we first

determined whether the LPA receptor antagonist Ki16425 inhibited LPA's ability to prevent

PMLF apoptosis. This antagonist was originally reported to inhibit LPA-induced responses

mediated by LPA$_1$ $\geq$ LPA$_3$ $>>$ LPA$_2$ (35), but more recent studies have demonstrated that the

ability of Ki16425 to inhibit mouse LPA$_1$ is over 10-fold greater than its ability to inhibit mouse

LPA$_3$, as assessed by calcium flux assays performed with transfected cells (personal

communication, Gretchen Bain, Amira Pharmaceuticals, San Diego, CA). The ability of LPA to

prevent PMLF apoptosis induced by serum deprivation was completely abrogated by Ki16425 at

a concentration of 100 μM (Figure 6B), and partially blocked by lower concentrations of

Ki16425 (Supplemental Figure E9), consistent with the anti-apoptotic effects of LPA on

fibroblasts being mediated by LPA$_1$. We next investigated whether LPA was able to prevent the

apoptosis of PMLF isolated from LPA$_1$ KO mice. As demonstrated in Figure 6C, LPA did not

significantly reduce the apoptosis of LPA$_1$ KO PMLF induced by serum deprivation for 24

hours, also suggesting that signaling through LPA$_1$ mediates the anti-apoptotic effects of LPA on

fibroblasts. In all the fibroblast experiments described above, PMLF were grown on high

attachment tissue culture-treated plastic. To determine whether LPA's ability to prevent lung

fibroblast apoptosis requires cell attachment, we investigated whether LPA was able to prevent

apoptosis of PMLF transferred to ultra low attachment plastic. As demonstrated in Figure 6D,

incubation with either serum or LPA each failed to reduce the apoptosis of PMLF on ultra low

attachment plastic. These results suggest that, as was the case for epithelial cells, LPA regulates

the apoptosis of fibroblasts only when these cells are adherent, and not when they are unattached.

DISCUSSION

We previously demonstrated that LPA signaling through LPA$_1$ importantly contributes to the development of bleomycin-induced pulmonary fibrosis (2), finding that LPA$_1$ KO mice are dramatically protected from fibrosis and mortality in this model. In this prior work, we demonstrated that LPA-LPA$_1$ signaling contributes to fibroblast recruitment and vascular leak induced by bleomycin challenge. In the current study, we have described two additional mechanisms through which this signaling pathway may contribute to fibrosis induced by bleomycin lung injury: LPA signaling through LPA$_1$ promotes lung epithelial cell apoptosis but fibroblast resistance to apoptosis. LPA-LPA$_1$ signaling thus could contribute to the paradoxical apoptotic abnormalities observed in IPF, in which increased epithelial but reduced fibroblast apoptosis may each play important roles in the development of fibrosis (36).

We found that the early wave of alveolar and bronchial epithelial cell apoptosis induced by bleomycin injury was attenuated in LPA$_1$ KO mice, suggesting that LPA signaling through LPA$_1$ promotes apoptosis in both the alveolar and bronchial epithelia after lung injury. Following an increase in BAL LPA concentration noted at day 1 post-bleomycin challenge, significantly increased numbers of TUNEL$^+$ alveolar and bronchial epithelial cells were present in WT compared to LPA$_1$ KO mice at day 3 post-challenge.

To investigate whether LPA-LPA$_1$ signaling could promote lung epithelial cell apoptosis by acting directly on these cells, we determined the effects of LPA on NHBE and R3/1 rat alveolar epithelial cell line cells in culture. As noted, we found in our *in vivo* studies that LPA-LPA$_1$ signaling promoted apoptosis in the alveolar and bronchial epithelia to similar extents and with similar kinetics, suggesting that these primary bronchial epithelial cells are a relevant *in*

vitro model in which to investigate the effects of LPA-LPA_1 signaling on epithelial cells. We found that LPA signaling through LPA_1 induced the apoptosis of subconfluent NHBE cells grown on matrigel, used as representative of basement membrane proteins normally present in the lung prior to injury or fibrosis. We found evidence that LPA-LPA_1 signaling specifically mediates lung epithelial cell anoikis, the apoptosis of anchorage-dependent cells induced by their detachment (30). Mediators that promote anoikis can do so either by promoting cell detachment or by promoting the apoptosis of cells once they have become detached. We found that LPA specifically induced NHBE cell detachment, but did not influence the rate at which cells became apoptotic once they were detached. Consistent with this mechanism of apoptosis induction, we found that LPA inhibited NHBE cell formation of focal adhesions and actin stress fibers, both of which structures have been demonstrated to transmit survival signals in adherent cells (32) (33). We found that LPA had similar effects on R3/1 cell attachment as it did on NHBE attachment, suggesting that LPA negatively regulates the attachment of both alveolar and bronchial epithelial cells, although we have not investigated primary alveolar epithelial cells.

Anoikis is thought to play important roles in normal development and tissue homeostasis, and abnormalities of this apoptotic pathway have been implicated in several disease processes (37). Development of resistance to anoikis is a crucial step during tumorigenesis, required for tumor cell anchorage-independent growth and metastatic spread. In contrast, evidence for increased apoptosis due to disruption of survival signals transmitted from ECM proteins has been reported in the development of renal fibrosis in glomerulosclerotic diseases such as lupus nephritis and IgA nephropathy (38). Aberrant induction of mesangial cell apoptosis after renal injury appears to contribute to the development of progressive fibrosis in these diseases, and has

been hypothesized to result from injury-induced changes in ECM composition, in which ECM proteins unable to suppress mesangial cell apoptosis are upregulated (39).

Since the discovery that LPA is a potent signaling molecule involved in a wide variety of basic physiological and pathological processes, multiple investigators have reported that LPA can promote either the survival or apoptosis of many different cell types (4). Consistent with our finding that LPA promotes lung epithelial cell anoikis, LPA$_1$ signaling has previously been shown to promote anoikis of other cell types, including ovarian epithelial cancer cells (40). In contrast to our results with epithelial cells, we found that LPA signaling through LPA$_1$ promoted the survival of primary mouse lung fibroblasts, consistent with previously reported findings that LPA prevents apoptosis of NIH 3T3, Swiss 3T3, and Rat-1 fibroblast cell lines (34), as well as other cell lineages such as Schwann cells (41). Interestingly, whereas we found LPA's ability to promote epithelial cell apoptosis was associated with inhibition of focal adhesion and actin stress fiber formation in these cells, LPA's ability to prevent Schwann cell apoptosis was associated with promotion of Schwann cell focal adhesion assembly and actin rearrangement (42).

There is evidence to suggest that lung fibroblasts in IPF are abnormally resistant to apoptosis (12). Fibroblast resistance to apoptosis coupled with increased epithelial cell apoptosis has been referred to as an "apoptosis paradox" in IPF (36). The molecular pathways responsible for the divergent susceptibilities of epithelial cells and fibroblasts to apoptosis in IPF have yet to be fully identified, but our data suggests that LPA signaling through LPA$_1$ may contribute. There is precedent for both epithelial cell apoptosis and fibroblast resistance to apoptosis being induced by the same mediator, as we propose for LPA. TGF-β has been shown to produce divergent apoptotic behaviors in different cell types and stimulation contexts (43). As we found with LPA, TGF-β induces apoptosis of lung epithelial cells (44, 45), but induces resistance to

apoptosis in lung fibroblasts (46, 47). Recently PGE_2 has also been shown to mediate divergent effects on lung epithelial cell and fibroblast apoptosis, but in the directions opposite to LPA and TGF-β. PGE_2 was found to promote the apoptosis of primary IPF lung fibroblasts, but to protect primary fibrotic lung type II cells against apoptosis (48). Therefore, increased LPA levels (2), increased TGF-β levels and/or activity (49) and decreased PGE_2 levels (50) in the lung in IPF may each contribute to the increased epithelial cell but reduced fibroblast apoptosis observed in this disease.

In this study, we have demonstrated that LPA signaling through its receptor LPA_1 promotes epithelial cell apoptosis induced by lung injury. Mechanistically, LPA appears to induce epithelial cell anoikis by promoting the detachment of these cells. In contrast, LPA-LPA_1 signaling promotes fibroblast resistance to apoptosis. In addition to the reductions in fibroblast recruitment and vascular leak that we previously observed in bleomycin-challenged LPA_1 KO mice, concurrent reductions in both epithelial cell apoptosis and fibroblast resistance to apoptosis may further explain the dramatic protection of these mice from fibrosis and mortality in the bleomycin model of pulmonary fibrosis. These new findings may have implications for therapeutic targeting of LPA-LPA_1 signaling in IPF. Antagonism of LPA_1 may be able to not only slow the development of new areas of fibrosis by reducing epithelial cell apoptosis, it may also be able to reverse the progression of established areas of fibrosis by promoting fibroblast apoptosis. Contributions of LPA and LPA_1 to the "apoptosis paradox" of IPF therefore highlight the potential of this signaling pathway to be a new therapeutic target for this devastating disease.

REFERENCES

1.   Selman M, King TE, Pardo A. Idiopathic pulmonary fibrosis: Prevailing and evolving hypotheses about its pathogenesis and implications for therapy. *Ann Intern Med* 2001;134(2):136-151.

2.   Tager AM, LaCamera P, Shea BS, Campanella GS, Selman M, Zhao Z, Polosukhin V, Wain J, Karimi-Shah BA, Kim ND, Hart WK, Pardo A, Blackwell TS, Xu Y, Chun J, Luster AD. The lysophosphatidic acid receptor LPA1 links pulmonary fibrosis to lung injury by mediating fibroblast recruitment and vascular leak. *Nat Med* 2008;14(1):45-54.

3.   Choi JW, Herr DR, Noguchi K, Yung YC, Lee CW, Mutoh T, Lin ME, Teo ST, Park KE, Mosley AN, Chun J. LPA receptors: Subtypes and biological actions. *Annu Rev Pharmacol Toxicol*;50:157-186.

4.   Ye X, Ishii I, Kingsbury MA, Chun J. Lysophosphatidic acid as a novel cell survival/apoptotic factor. *Biochim Biophys Acta* 2002;1585(2-3):108-113.

5.   Kuwano K, Kunitake R, Kawasaki M, Nomoto Y, Hagimoto N, Nakanishi Y, Hara N. P21Waf1/Cip1/Sdi1 and p53 expression in association with DNA strand breaks in idiopathic pulmonary fibrosis. *Am J Respir Crit Care Med* 1996;154(2 Pt 1):477-483.

6.   Plataki M, Koutsopoulos AV, Darivianaki K, Delides G, Siafakas NM, Bouros D. Expression of apoptotic and antiapoptotic markers in epithelial cells in idiopathic pulmonary fibrosis. *Chest* 2005;127(1):266-274.

7.   Hagimoto N, Kuwano K, Miyazaki H, Kunitake R, Fujita M, Kawasaki M, Kaneko Y, Hara N. Induction of apoptosis and pulmonary fibrosis in mice in response to ligation of Fas antigen. *Am J Respir Cell Mol Biol* 1997;17(3):272-278.

8.   Matute-Bello G, Wurfel MM, Lee JS, Park DR, Frevert CW, Madtes DK, Shapiro SD, Martin TR. Essential role of MMP-12 in Fas-induced lung fibrosis. *Am J Respir Cell Mol Biol* 2007;37(2):210-221.

9.   Lee CG, Cho SJ, Kang MJ, Chapoval SP, Lee PJ, Noble PW, Yehualaeshet T, Lu B, Flavell RA, Milbrandt J, Homer RJ, Eias JA. Early growth response gene 1-mediated apoptosis is essential for transforming growth factor beta1-induced pulmonary fibrosis. *J Exp Med* 2004;200(3):377-389.

10.   Sisson TH, Mendez M, Choi K, Subbotina N, Courey A, Cunningham A, Dave A, Engelhardt JF, Liu X, White ES, Thannikal VJ, Moore BB, Christensen PJ, Simon RH. Targeted injury of type II alveolar epithelial cells induces pulmonary fibrosis. *Am J Respir Crit Care Med* 2010;181(3):254-263.

11.   Hagimoto N, Kuwano K, Nomoto Y, Kunitake R, Hara N. Apoptosis and expression of Fas/Fas ligand mRNA in bleomycin-induced pulmonary fibrosis in mice. *Am J Respir Cell Mol Biol* 1997;16(1):91-101.

12.   Chang W, Wei K, Jacobs SS, Upadhyay D, Weill D, Rosen GD. SPARC suppresses apoptosis of idiopathic pulmonary fibrosis fibroblasts through constitutive activation of beta-catenin. *J Biol Chem*;285(11):8196-8206.

13.   Funke M, Shea BS, Groom J, Castelino F, Brooks SF, Chun J, Tager AM. Lysophosphatidic acid contributes to an apoptosis paradox in lung fibrosis. *Am J Respir Crit Care Med* 2009(179):A1988.

14.   Contos JJ, Fukushima N, Weiner JA, Kaushal D, Chun J. Requirement for the LPA1 lysophosphatidic acid receptor gene in normal suckling behavior. *Proc Natl Acad Sci U S A* 2000;97(24):13384-13389.

15.   Xiao YJ, Schwartz B, Washington M, Kennedy A, Webster K, Belinson J, Xu Y. Electrospray ionization mass spectrometry analysis of lysophospholipids in human ascitic fluids: Comparison of the lysophospholipid contents in malignant vs nonmalignant ascitic fluids. *Anal Biochem* 2001;290(2):302-313.

16.   Knebel JW, Aufderheide M, Emura M. Comparison of biological effects of different polycyclic aromatic hydrocarbons in lung cells of hamster and rat in vitro. *Toxicol Lett* 1994;72(1-3):65-72.

17.   Koslowski R, Barth K, Augstein A, Tschernig T, Bargsten G, Aufderheide M, Kasper M. A new rat type I-like alveolar epithelial cell line R3/1: Bleomycin effects on caveolin expression. *Histochem Cell Biol* 2004;121(6):509-519.

18.   Tager AM, Kradin RL, LaCamera P, Bercury SD, Campanella GS, Leary CP, Polosukhin V, Zhao LH, Sakamoto H, Blackwell TS, Luster AD. Inhibition of pulmonary fibrosis by the chemokine IP-10/CXCL10. *Am J Respir Cell Mol Biol* 2004;31(4):395-404.

19.   Kuwano K, Hagimoto N, Tanaka T, Kawasaki M, Kunitake R, Miyazaki H, Kaneko Y, Matsuba T, Maeyama T, Hara N. Expression of apoptosis-regulatory genes in epithelial cells in pulmonary fibrosis in mice. *J Pathol* 2000;190(2):221-229.

20.   Kuwano K, Kunitake R, Maeyama T, Hagimoto N, Kawasaki M, Matsuba T, Yoshimi M, Inoshima I, Yoshida K, Hara N. Attenuation of bleomycin-induced pneumopathy in mice by a caspase inhibitor. *Am J Physiol Lung Cell Mol Physiol* 2001;280(2):L316-325.

21.   Dobbs LG, Williams MC, Gonzalez R. Monoclonal antibodies specific to apical surfaces of rat alveolar type I cells bind to surfaces of cultured, but not freshly isolated, type II cells. *Biochim Biophys Acta* 1988;970(2):146-156.

22.   Savani RC, Godinez RI, Godinez MH, Wentz E, Zaman A, Cui Z, Pooler PM, Guttentag SH, Beers MF, Gonzales LW, Ballard PL. Respiratory distress after intratracheal bleomycin: Selective deficiency of surfactant proteins B and C. *Am J Physiol Lung Cell Mol Physiol* 2001;281(3):L685-696.

23.   Zhao Z, Xu Y. Measurement of endogenous lysophosphatidic acid by ESI-MS/MS in plasma samples requires pre-separation of lysophosphatidylcholine. *J Chromatogr B Analyt Technol Biomed Life Sci* 2009;877(29):3739-3742.

24.   Moore A, Donahue CJ, Bauer KD, Mather JP. Simultaneous measurement of cell cycle and apoptotic cell death. *Methods Cell Biol* 1998;57:265-278.

25.   Kim KK, Kugler MC, Wolters PJ, Robillard L, Galvez MG, Brumwell AN, Sheppard D, Chapman HA. Alveolar epithelial cell mesenchymal transition develops in vivo during pulmonary fibrosis and is regulated by the extracellular matrix. *Proc Natl Acad Sci U S A* 2006;103(35):13180-13185.

26.   Ramsey WS, Hertl W, Nowlan ED, Binkowski NJ. Surface treatments and cell attachment. *In Vitro* 1984;20(10):802-808.

27.   Medoff BD, Landry AL, Wittbold KA, Sandall BP, Derby MC, Cao Z, Adams JC, Xavier RJ. CARMA3 mediates lysophosphatidic acid-stimulated cytokine secretion by bronchial epithelial cells. *Am J Respir Cell Mol Biol* 2009;40(3):286-294.

28.   Castelino FV, Seiders J, Bain G, Brooks SF, King C, Swaney JS, Lorrain DS, Chun J, Luster AD, Tager AM. Genetic deletion or pharmacologic antagonism of LPA(1) ameliorates dermal fibrosis in a scleroderma mouse model. *Arthritis Rheum.*

29.   Swaney JS, Chapman C, Correa LD, Stebbins KJ, Broadhead AR, Bain G, Santini AM, Darlington J, King CD, Baccei C, Lee C, Parr TA, Roppe JR, Seiders TJ, Ziff J, Prasit P, Hutchinson JH, Evans JF, Lorrain DS. Pharmacokinetic and pharmacodynamic characterization of an oral, LPA1-selective antagonist. *J Pharmacol Exp Ther* 2010.

30.   Frisch SM, Francis H. Disruption of epithelial cell-matrix interactions induces apoptosis. *J Cell Biol* 1994;124(4):619-626.

31.   Gilmore AP. Anoikis. *Cell Death Differ* 2005;12 Suppl 2:1473-1477.

32.   Gilmore AP, Owens TW, Foster FM, Lindsay J. How adhesion signals reach a mitochondrial conclusion-ECM regulation of apoptosis. *Curr Opin Cell Biol* 2009;21(5):654-661.

33.   Cheng TL, Symons M, Jou TS. Regulation of anoikis by Cdc42 and Rac1. *Exp Cell Res* 2004;295(2):497-511.

34.   Fang X, Yu S, LaPushin R, Lu Y, Furui T, Penn LZ, Stokoe D, Erickson JR, Bast RC, Jr., Mills GB. Lysophosphatidic acid prevents apoptosis in fibroblasts via G(i)-protein-mediated activation of mitogen-activated protein kinase. *Biochem J* 2000;352 Pt 1:135-143.

35.   Ohta H, Sato K, Murata N, Damirin A, Malchinkhuu E, Kon J, Kimura T, Tobo M, Yamazaki Y, Watanabe T, Yagi M, Sato M, Suzuki R, Murooka H, Sakai T, Nishitoba T, Im DS, Nochi H, Tamoto K, Tomura H, Okajima F. Ki16425, a subtype-selective antagonist for EDG-family lysophosphatidic acid receptors. *Mol Pharmacol* 2003;64(4):994-1005.

36.   Thannickal VJ, Horowitz JC. Evolving concepts of apoptosis in idiopathic pulmonary fibrosis. *Proc Am Thorac Soc* 2006;3(4):350-356.

37.   Chiarugi P, Giannoni E. Anoikis: A necessary death program for anchorage-dependent cells. *Biochem Pharmacol* 2008;76(11):1352-1364.

38.   Makino H, Sugiyama H, Kashihara N. Apoptosis and extracellular matrix-cell interactions in kidney disease. *Kidney Int Suppl* 2000;77:S67-75.

39.   Mooney A, Jackson K, Bacon R, Streuli C, Edwards G, Bassuk J, Savill J. Type IV collagen and laminin regulate glomerular mesangial cell susceptibility to apoptosis via beta(1) integrin-mediated survival signals. *Am J Pathol* 1999;155(2):599-606.

40.   Furui T, LaPushin R, Mao M, Khan H, Watt SR, Watt MA, Lu Y, Fang X, Tsutsui S, Siddik ZH, Bast RC, Mills GB. Overexpression of edg-2/vzg-1 induces apoptosis and anoikis in ovarian cancer cells in a lysophosphatidic acid-independent manner. *Clin Cancer Res* 1999;5(12):4308-4318.

41.   Weiner JA, Chun J. Schwann cell survival mediated by the signaling phospholipid lysophosphatidic acid. *Proc Natl Acad Sci U S A* 1999;96(9):5233-5238.

42.   Weiner JA, Fukushima N, Contos JJ, Scherer SS, Chun J. Regulation of schwann cell morphology and adhesion by receptor-mediated lysophosphatidic acid signaling. *J Neurosci* 2001;21(18):7069-7078.

43.   Rahimi RA, Leof EB. TGF-beta signaling: A tale of two responses. *J Cell Biochem* 2007;102(3):593-608.

44.   Hagimoto N, Kuwano K, Inoshima I, Yoshimi M, Nakamura N, Fujita M, Maeyama T, Hara N. TGF-beta 1 as an enhancer of Fas-mediated apoptosis of lung epithelial cells. *J Immunol* 2002;168(12):6470-6478.

45.   Solovyan VT, Keski-Oja J. Proteolytic activation of latent TGF-beta precedes caspase-3 activation and enhances apoptotic death of lung epithelial cells. *J Cell Physiol* 2006;207(2):445-453.

46.   Zhang HY, Phan SH. Inhibition of myofibroblast apoptosis by transforming growth factor beta(1). *Am J Respir Cell Mol Biol* 1999;21(6):658-665.

47.   Horowitz JC, Rogers DS, Sharma V, Vittal R, White ES, Cui Z, Thannickal VJ. Combinatorial activation of Fak and Akt by transforming growth factor-beta1 confers an anoikis-resistant phenotype to myofibroblasts. *Cell Signal* 2007;19(4):761-771.

48.   Maher TM, Evans IC, Bottoms SE, Mercer PF, Thorley AJ, Nicholson AG, Laurent GJ, Tetley TD, Chambers RC, McAnulty RJ. Diminished prostaglandin E2 contributes to the apoptosis paradox in idiopathic pulmonary fibrosis. *Am J Respir Crit Care Med* 2010 Jul 1;182(1):73-82.

49.   Coker RK, Laurent GJ, Jeffery PK, du Bois RM, Black CM, McAnulty RJ. Localisation of transforming growth factor beta1 and beta3 mRNA transcripts in normal and fibrotic human lung. *Thorax* 2001;56(7):549-556.

50.   Borok Z, Gillissen A, Buhl R, Hoyt RF, Hubbard RC, Ozaki T, Rennard SI, Crystal RG. Augmentation of functional prostaglandin E levels on the respiratory epithelial surface by aerosol administration of prostaglandin E. *Am Rev Respir Dis* 1991;144(5):1080-1084.

FIGURE LEGENDS

Figure 1. Bleomycin-induced alveolar epithelial apoptosis was attenuated in LPA_1 KO mice. (A – C) The increase in TUNEL$^+$ cells induced by bleomycin in the alveolar epithelium was attenuated in LPA_1 KO mice. Representative TUNEL/peroxidase-stained sections of (A) WT and (B) LPA_1 KO mouse lungs 3 days after bleomycin challenge. Scale bars = 50 μm for all images. (C) Mean numbers of TUNEL$^+$ cells per high power field ± SEM in lung sections of WT and LPA_1 KO mice at day 0, 1, 3 and 5 post-bleomycin. Data were pooled from two independent experiments; the combined numbers of samples were n = 3 (day 0) or 6 (days 1, 3 and 5) for WT and LPA_1 KO mice. $**P < 0.01$, WT vs. LPA_1 KO mice at day 3 post-challenge; significance for this comparison, and for all subsequent comparisons performed for experiments with only two experimental groups, was determined by two-tailed Student's T-test. (D – F) The increase in p53$^+$ cells induced by bleomycin in the alveolar epithelium was attenuated in LPA_1 KO mice. Representative p53/peroxidase-stained sections of (D) WT and (E) LPA_1 KO mouse lungs 3 days after bleomycin challenge. (F) Mean numbers of p53$^+$ cells per high power field ± SEM in WT and LPA_1 KO lung sections at day 0 and 3 post-bleomycin, n = 3 (day 0) or 7 (day 3) for each genotype. $**P = 0.01$, WT vs. LPA_1 KO mice at day 3. (G – I) The increase in p21$^+$ cells induced by bleomycin in the alveolar epithelium was attenuated in LPA_1 KO mice. Representative images of p21/peroxidase-stained sections of (G) WT and (H) LPA_1 KO mouse lungs 3 days after bleomycin challenge. (I) Mean numbers of p21$^+$ cells per high power field ± SEM in WT and LPA_1 KO lung sections at day 0 and 3 post-bleomycin, n = 3 (day 0) or 7 (day 3) for each genotype. $^{\#}P < 0.001$, WT vs. LPA_1 KO mice at day 3. (J) Mean caspase 3 activity / whole lung set ± SEM measured in WT and LPA_1 KO lung homogenates at day 0 and 3 post-

bleomycin, n = 7 to 10 for each genotype at each time point. **P = 0.01, WT vs. LPA$_1$ KO mice

at day 3.

Figure 2. Bleomycin-induced bronchial epithelial apoptosis was attenuated in LPA$_1$ KO

mice. The increase in TUNEL$^+$ cells induced by bleomycin in the bronchial epithelium was

attenuated of LPA$_1$ KO mice. Representative TUNEL/peroxidase-stained sections of WT and

LPA$_1$ KO mouse lungs at day 0 (A, B), day 1 (C, D) and day 3 (E, F) after bleomycin challenge.

Scale bars = 50 μm for all images. (G) Mean numbers of TUNEL$^+$ cells per high power field ±

SEM in lung sections of WT and LPA$_1$ KO mice at day 0, 1 and 3 post-bleomycin. Data were

pooled from two independent experiments; the combined numbers of samples were n = 3 (day 0)

or 6 (days 1 and 3) for WT and LPA$_1$ KO mice. $^#P$ < 0.001, WT vs. LPA$_1$ KO mice at day 3

post-challenge.

Figure 3. Bleomycin increased LPA levels early after injury. (A) Mean concentrations of 6

LPA species (16:0, 18:0, 18:1, 18:2, 20:4 and 22:6 LPA) and (B) mean total LPA concentrations

in BAL of C57Bl/6 mice at day 0, 1 and 3 post-bleomycin. Three independent experiments were

performed. Data represent the means of the values produced in the individual experiments ±

SEM; the values produced in the individual experiments themselves were the means of n = 5

mice per time point. Significant differences are indicated as follows: *P < 0.05, **P < 0.01 and

$^{##}P$ < 0.0001. Significance for these comparisons, and for all subsequent comparisons performed

for experiments with more than two experimental groups, was determined by pairwise

comparisons made with Bonferroni post-test corrections after one-way ANOVA rejected the

hypothesis of equality of the group means.

Figure 4. LPA signaling through LPA_1 promoted lung epithelial cell apoptosis. (A) LPA (18:1) induced the apoptosis of normal human bronchial epithelial (NHBE) cells grown on matrigel. Apoptotic cells were identified by flow cytometry following staining with annexin V and propidium iodide (24), as annexin V-positive, PI-negative cells. Data from one of three independent experiments are presented as mean percentages of annexin V(+) PI(-) cells ± SEM, n = 3 cultures per treatment condition in each experiment. **$P < 0.01$, LPA-treated vs. untreated NHBE cells. (B) LPA (18:1) dose-dependently induced the apoptosis of NHBE cells grown on low attachment polystyrene. Four independent experiments were performed. Data are presented as mean fold increases in percentages of apoptotic [annexin V(+), PI(-)] cells in LPA-treated NHBE cells compared to untreated cells from the four individual experiments ± SEM; the values produced in the individual experiments themselves were the means of n = 3 cultures per treatment condition. *$P < 0.05$, [#]$P < 0.001$ and [##]$P < 0.0001$, NHBE cells treated with 1, 10 or 20µM LPA respectively vs. untreated cells. (C) LPA (18:0) also induced NHBE cell apoptosis, and this effect was abrogated by AM095, a selective LPA_1 receptor antagonist. Data are from a representative experiment with n = 3 cultures per treatment condition. [##]$P < 0.0001$, LPA-treated vs. untreated NHBE cells and AM095-treated LPA-treated NHBE cells vs. LPA-treated NHBE cells.

Figure 5. LPA promoted detachment and limited attachment of lung epithelial cells.
(A) LPA promoted detachment of NHBE cells from low attachment untreated polystyrene. Six independent experiments were performed. Data represent the means of the adherence indices produced in the individual experiments ± SEM; the values produced in the individual

experiments themselves were the means of n = 9 cultures per treatment condition. *$P < 0.05$, LPA-treated vs. untreated NHBE cells. (B) LPA limited attachment of NHBE cells to high attachment tissue culture-treated polystyrene. Four independent experiments were performed. Data represent the means of the percentages of spread cells produced in the individual experiments ± SEM; the values produced in the individual experiments themselves were the means of n = 3 cultures per treatment condition. Spread cells were identified visually by phase contrast microscopy as having flattened from their initial rounded shape such that the nucleus and cytoplasm could be differentiated. #$P < 0.001$, LPA-treated vs. untreated NHBE cells. (C, D) LPA limited NHBE cells formation of focal adhesions. Representative NHBE cells labeled with anti-vinculin-FITC 3 hours after transfer onto high attachment tissue culture-treated permanox slides (C) without LPA treatment and (D) with LPA treatment. (E, F) LPA limited NHBE cells formation of actin stress fibers. Representative NHBE cells labeled with fluorescein-phalloidin 3 hours after transfer onto high attachment permanox (E) without LPA treatment and (F) with LPA treatment. (G) LPA did not promote the apoptosis of NHBE cells transferred to ultra low attachment polystyrene plates. Three independent experiments were performed. Data represent the means of the percentages of annexin V(+) PI(-) cells produced in the individual experiments ± SEM; the values produced in the individual experiments themselves were the means of n = 3 cultures per treatment condition. Differences between LPA-treated and untreated NHBE cells were not significant. (H) LPA limited attachment of R3/1 rat alveolar epithelial cell line cells to high attachment tissue culture-treated polystyrene. Data represent the mean percentages of spread cells produced in a representative experiment ± SEM, with n = 3 cultures per treatment condition. Spread cells were identified as in (B). *$P < 0.05$ and ##$P < 0.0001$, untreated R3/1 cells vs. R3/1 cells treated with 1 and 20 μM LPA, respectively.

Figure 6. LPA signaling through LPA_1 promotes lung fibroblast resistance to apoptosis.

(A) LPA promoted PMLF resistance to apoptosis induced by serum deprivation when these cells were grown on high attachment tissue culture-treated polystyrene. Apoptotic cells were identified by flow cytometry following staining with annexin V and propidium iodide (8), as annexin V-positive, PI-negative cells. Three independent experiments were performed. In all panels of this figure, data represent the means of the percentages of annexin V(+) PI(-) cells produced in the individual experiments ± SEM; the values produced in the individual experiments themselves were the means of n = 3 cultures per treatment condition. $^{\#\#}P \leq 0.0001$, serum-deprived PMLF vs. PMLF in serum, and serum-deprived PMLF treated with 1, 10 or 20μM LPA vs. untreated serum-deprived cells. (B) LPA-induced resistance to apoptosis of PMLF grown on high attachment polystyrene was abrogated by Ki16425. Three independent experiments were performed. $**P < 0.01$, serum-deprived PMLF vs. PMLF in serum; serum-deprived LPA-treated PMLF vs. untreated serum-deprived cells, and serum-deprived LPA-treated PMLF that were also treated with Ki16425 vs. serum-deprived LPA-treated PMLF. (C) LPA did not promote resistance to apoptosis of PMLF isolated from LPA_1 KO mice that was induced by serum deprivation when these cells were grown on high attachment polystyrene. Three independent experiments were performed. $*P < 0.05$, serum-deprived LPA_1 KO PMLF vs. LPA_1 KO PMLF in serum. Differences between LPA-treated and untreated serum-deprived LPA_1 KO PMLF were not significant. (D) LPA did not promote resistance to apoptosis of PMLF transferred to ultra low attachment polystyrene. Three independent experiments were performed. Differences between LPA-treated and untreated serum-deprived PMLF were not significant.
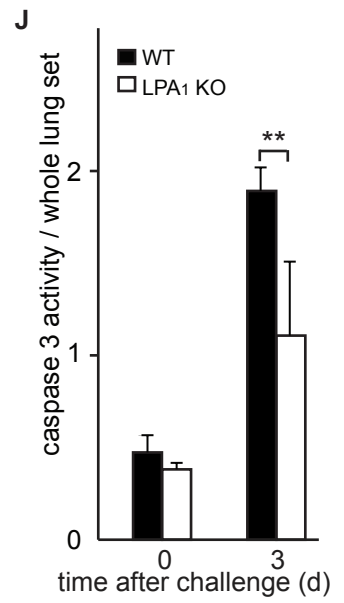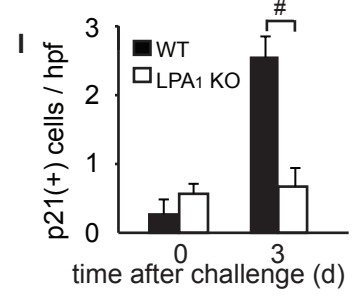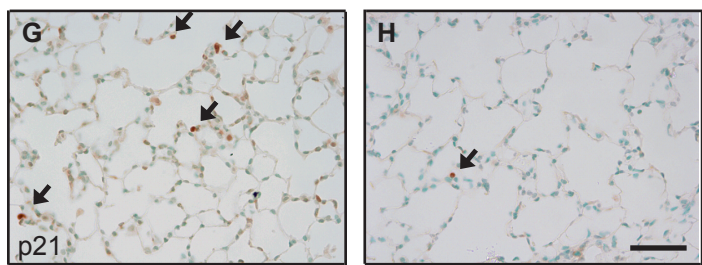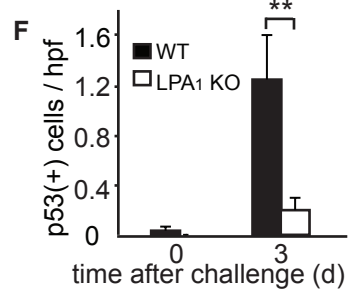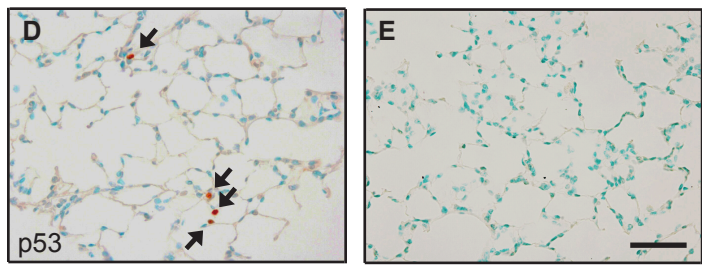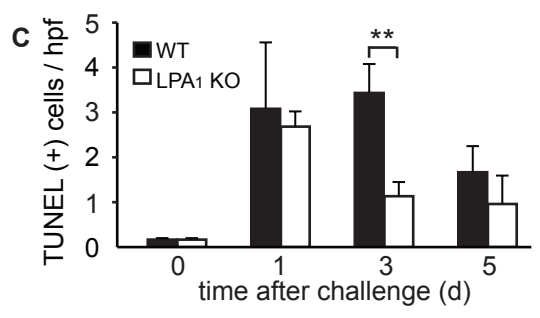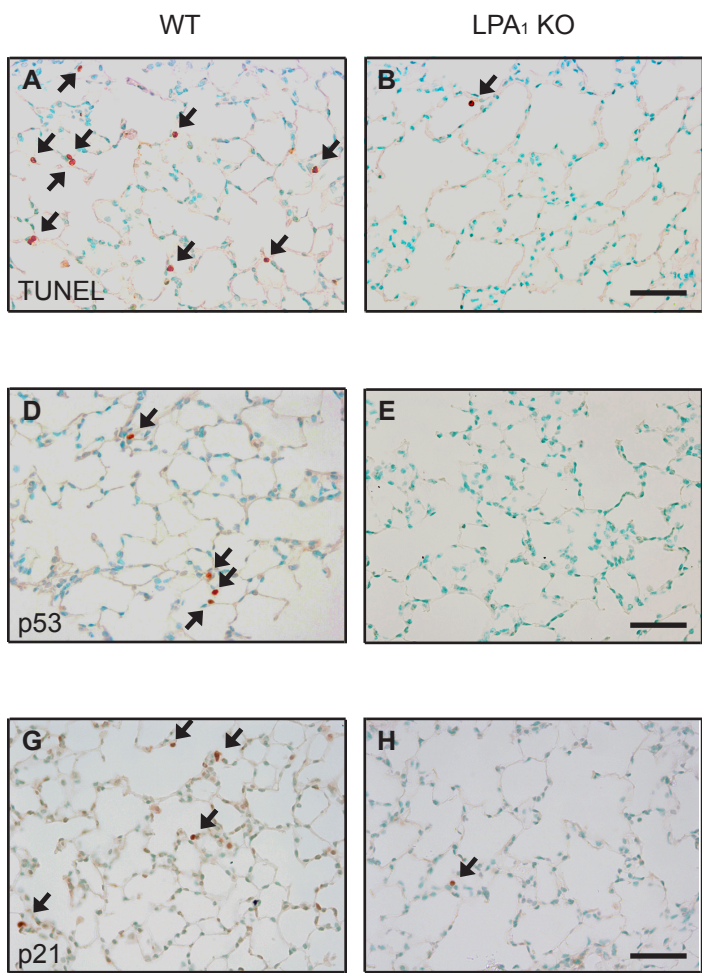
Figure 1
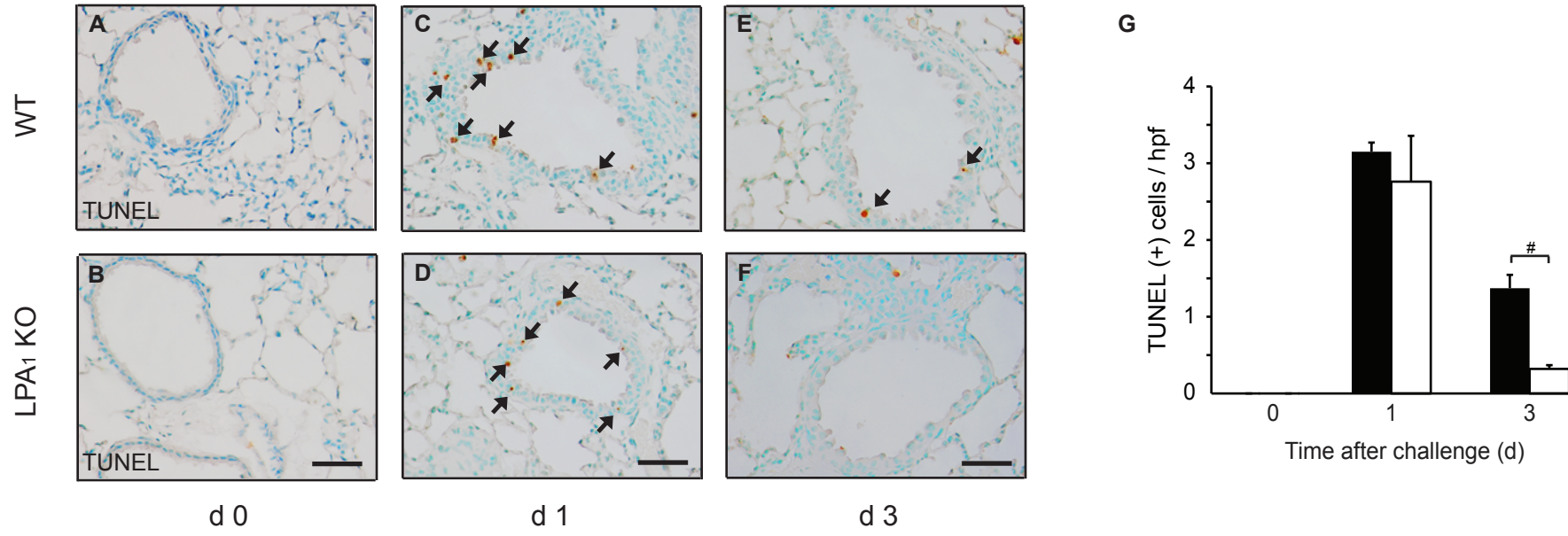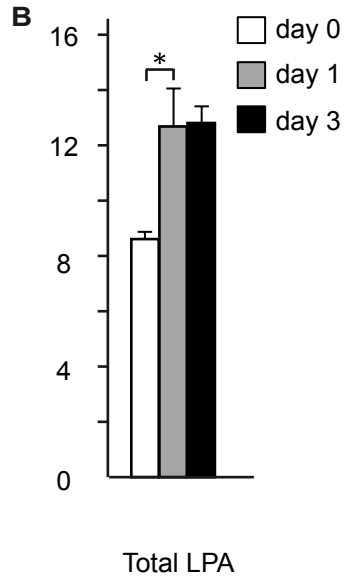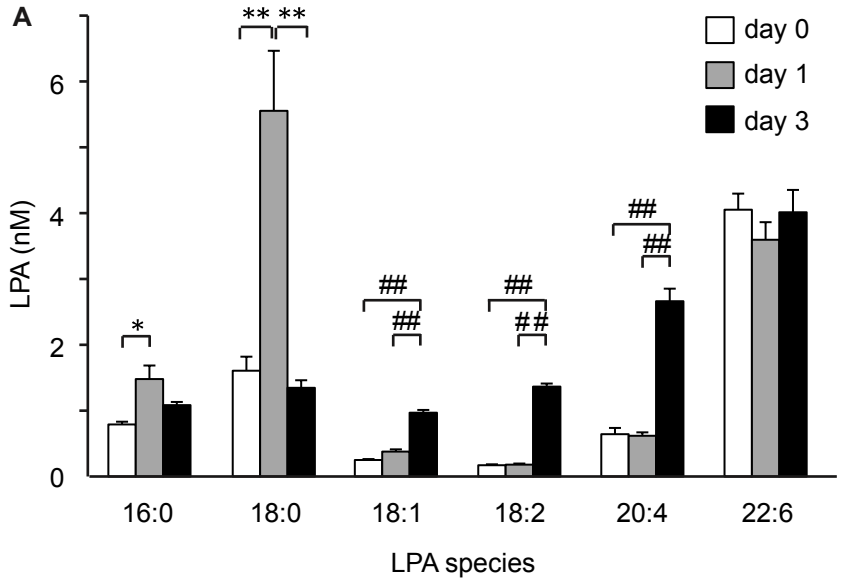
Figure 2

Figure 4

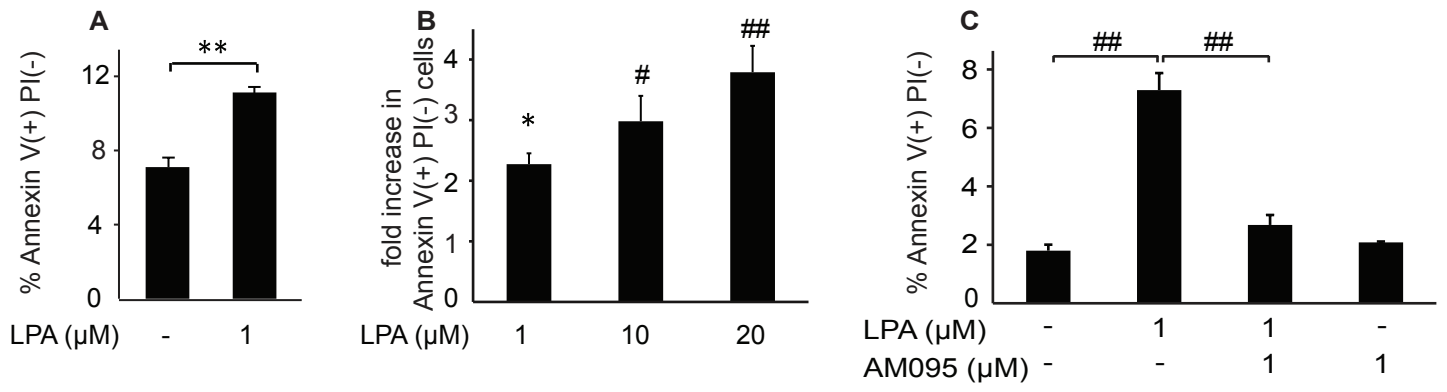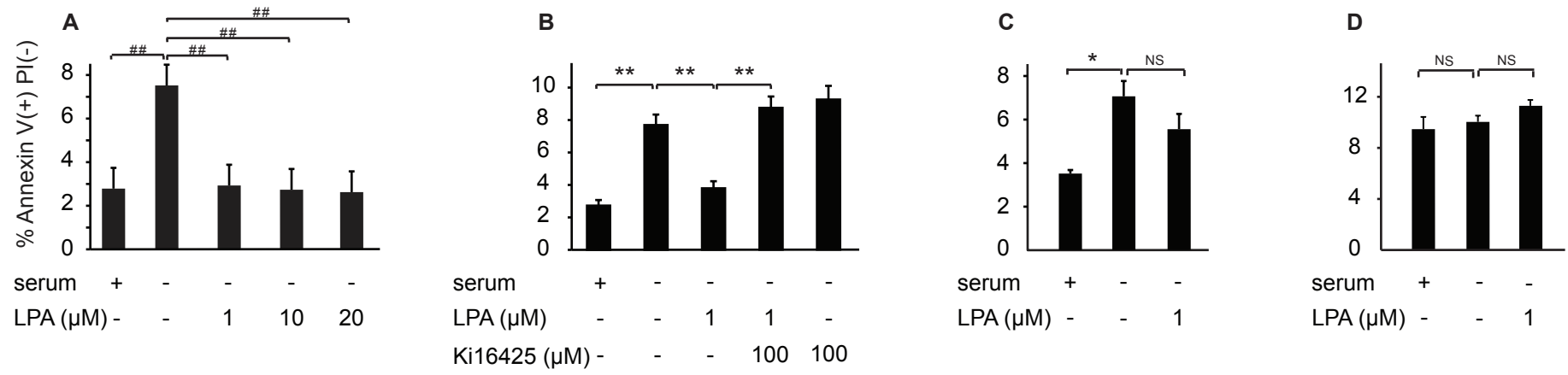**Figure 5**

Figure 6

ONLINE DATA SUPPLEMENT

The lysophosphosphatidic acid receptor LPA$_1$ promotes epithelial cell apoptosis following lung injury

Manuela Funke, Zhenwen Xhao, Yan Xu, Jerold Chun, and Andrew M. Tager

SUPPLEMENTAL MATERIAL AND METHODS

Lung immunohistochemical and immunofluorescence staining

Multiple paraffin-embedded 5 μm sections of the entire mouse lung were stained using the

Apoptag® peroxidase *in situ* apoptosis detection kit (Millipore, Billerica, MA, USA) according

to the manufacturer's instructions. Immunolabeling of p53 and p21 was performed with primary

rabbit anti-mouse p53 antibody (Santa Cruz Biotechnology, Santa Cruz, CA, USA) and primary

rabbit anti-mouse p21 antibody (Thermo Scientific, Waltham, MA, USA), respectively.

Appropriate biotinylated secondary antibodies were used, followed by detection with an ABC

Development Kit (Vector Laboratories, Burlingame, CA, USA) and color development with

DAB (Vector Laboratories). The numbers of $TUNEL^+$, $p53^+$ and $p21^+$ cells were determined by

counting the number of positive cells in 10 randomly selected non-overlapping high-power fields

in lung sections of WT and LPA_1 KO mice. For TUNEL co-staining with either T1α, a marker

of type I alveolar epithelial cells (AECs) (E1), or pro-surfactant protein C (proSP-C), a marker of

type II AECs, multiple paraffin-embedded 5 μm sections of the entire mouse lung were first

stained using the Apoptag® fluorescein direct *in situ* apoptosis detection kit (Millipore)

according to the manufacturer's instructions. Immunolabeling of T1α or pro-SPC on the same

sections was then performed with primary hamster anti-mouse T1α antibody (eBioscience, San

Diego, CA, USA) or primary rabbit anti-mouse pro-SPC antibody (Millipore), respectively.

Appropriate biotinylated secondary antibodies were used and labeled with Strepta-Alexa 555

(Invitrogen, Carlsbad, CA, USA), and sections were mounted with VECTASHIELD® mounting

medium with DAPI (Vector Laboratories).

NHBE, rat R3/1 and PMLF cell culture and apoptosis analysis

In different experiments evaluating normal human bronchial epithelial (NHBE) cell apoptosis, cells were transferred to Matrigel™ matrix thin layer 6 well multiwell plates (BD Bioscience, San Jose, CA, USA), Corning® 60mm not tissue culture (1)-treated culture dishes (low attachment dishes, Corning) or Corning® 6 well ultra low attachment culture plates (Corning). For NHBE cells transferred to matrigel, cells were cultured directly in bronchial epithelial cell growth medium (BEGM) with 0.1% fatty acid-free BSA (FAF-BSA, Sigma Aldrich, St. Louis, MO, USA) with or without 18:1 lysophosphatidic acid (LPA, Avanti Polar Lipids, Alabaster, AL, USA) for 48h prior to apoptosis analyses. For NHBE cells transferred to low attachment dishes, cells were cultured in BEGM without FAF-BSA or LPA for 24 h, and then in BEGM with FAF-BSA with or without either 18:1 or 18:0 LPA, and with or without AM095 (Amira Pharmaceuticals, San Diego, CA, USA) for 72h. For NHBE cells transferred to ultra low attachment dishes, cells were cultured directly in BEGM with FAF-BSA with or without 18:1 LPA for 24h. NHBE cells transferred to low attachment dishes were harvested with a cell lifter (Corning Costar) after incubation with 0.05% trypsin-EDTA (Cellgro, Manassas, VA, USA) for 1 min; cells transferred to matrigel were harvested after incubation with trypsin-EDTA without a cell lifter; cells transferred to ultra low attachment plates were harvested with pipetting only. Primary mouse lung fibroblasts (PMLF) for apoptosis assays transferred at passage 3 were transferred into MULTIWELL™ 6 well TC-treated polystyrene tissue culture plates (Falcon, BD Bioscience) or Corning® 6 well ultra low attachment culture plates. Transferred cells were cultured in DMEM with 15% FBS (DMEM-15%) for 24h, then washed twice with PBS, and then cultured in serum-free DMEM with 0.1% FAF-BSA with or without 18:1 LPA for 24h. PMLF were then harvested by incubation with 0.25% trypsin-EDTA for 1 min. Rat R3/1 cells

4

were cultured in supplemented DMEM (10%FBS) and used for experiments up to passage 10.

Harvest and LPA treatment of rat R3/1 cells was similar to the treatment of PMLFs. For all

experiments, cells were cultured at 37°C and 5% CO_2 in a humidified incubator. NHBE cells

and PMLF harvested for apoptosis analyses were incubated with FITC annexin V (BD

Bioscience) in buffer containing propidium iodide (PI, BD Bioscience) at room temperature for

15 min. Percentages of apoptotic cells, identified as annexin V-positive, PI-negative cells (E2),

were determined by cytofluorometry performed using a FACS Calibur Cytometer (BD

Bioscience) and analyzed using FlowJo® software (Tree Star, Ashland, OR, USA).

Cell Detachment and Attachment Assays

For detachment assays, NHBE cells were transferred into a Corning® 96 well flat bottom

polystyrene not TC-treated microplate (Corning) at 6,000 cells/well, and incubated in BEGM for

1h. FAF-BSA with or without 18:1 LPA was added to the wells, and the cells were incubated for

an additional 2h. The media was then aspirated and the plate was centrifuged in an inverted

position at 900 x g for 5min at 4°C. Cells remaining in the wells were then fixed with 5%

glutaraldehyde and stained with crystal violet (Sigma Aldrich). Wells were washed with tap

water followed by 10% acetic acid, and absorption of the remaining crystal violet was measured

at 570nm. Adherence indices were determined as absorption in wells in which cells had been

treated with FAF-BSA/LPA relative to wells in which cells had been treated with FAF-BSA

only. For attachment assays, NHBE or rat R3/1 cells were transferred into a MULTIWELL™ 96

well TC-treated flat bottom polystyrene tissue culture plate (Falcon, BD Bioscience) at 5,000

cells/well, and cultured directly in BEGM with FAF-BSA with or without LPA. Attached cells

were then identified after 3h as those that had spread, or flattened, as described (E3), and counted

in 10 randomly selected non-overlapping high-power fields.

SUPPLEMENTAL REFERENCES

E1.　　Swaney JS, Chapman C, Correa LD, Stebbins KJ, Broadhead AR, Bain G, Santini AM, Darlington J, King CD, Baccei C, et al. Pharmacokinetic and pharmacodynamic characterization of an oral, LPA1-selective antagonist. *J Pharmacol Exp Ther* 2011;336(3):693-700.

E2.　　Moore A, Donahue CJ, Bauer KD, Mather JP. Simultaneous measurement of cell cycle and apoptotic cell death. *Methods Cell Biol* 1998;57:265-278.

E3.　　Humphries MJ. Cell adhesion assays. *Methods Mol Biol* 2009;522:203-210.

Supplemental Figure E1
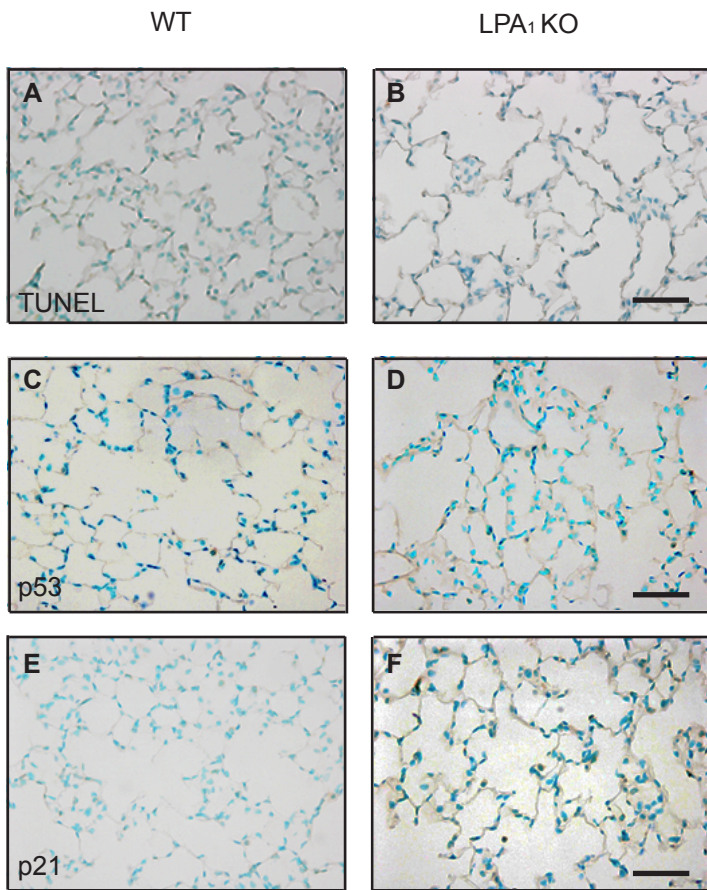
Figure E1. Minimal apoptosis was present in the lungs of WT and LPA$_1$ KO mice at baseline.
Representative (A, B) TUNEL/peroxidase-stained, (C, D) p53/peroxidase-stained, and (E, F) p21/peroxidase-stained sections of WT and LPA$_1$ KO mouse lungs at baseline prior to bleomycin challenge (day 0). Scale bars = 50 µm.
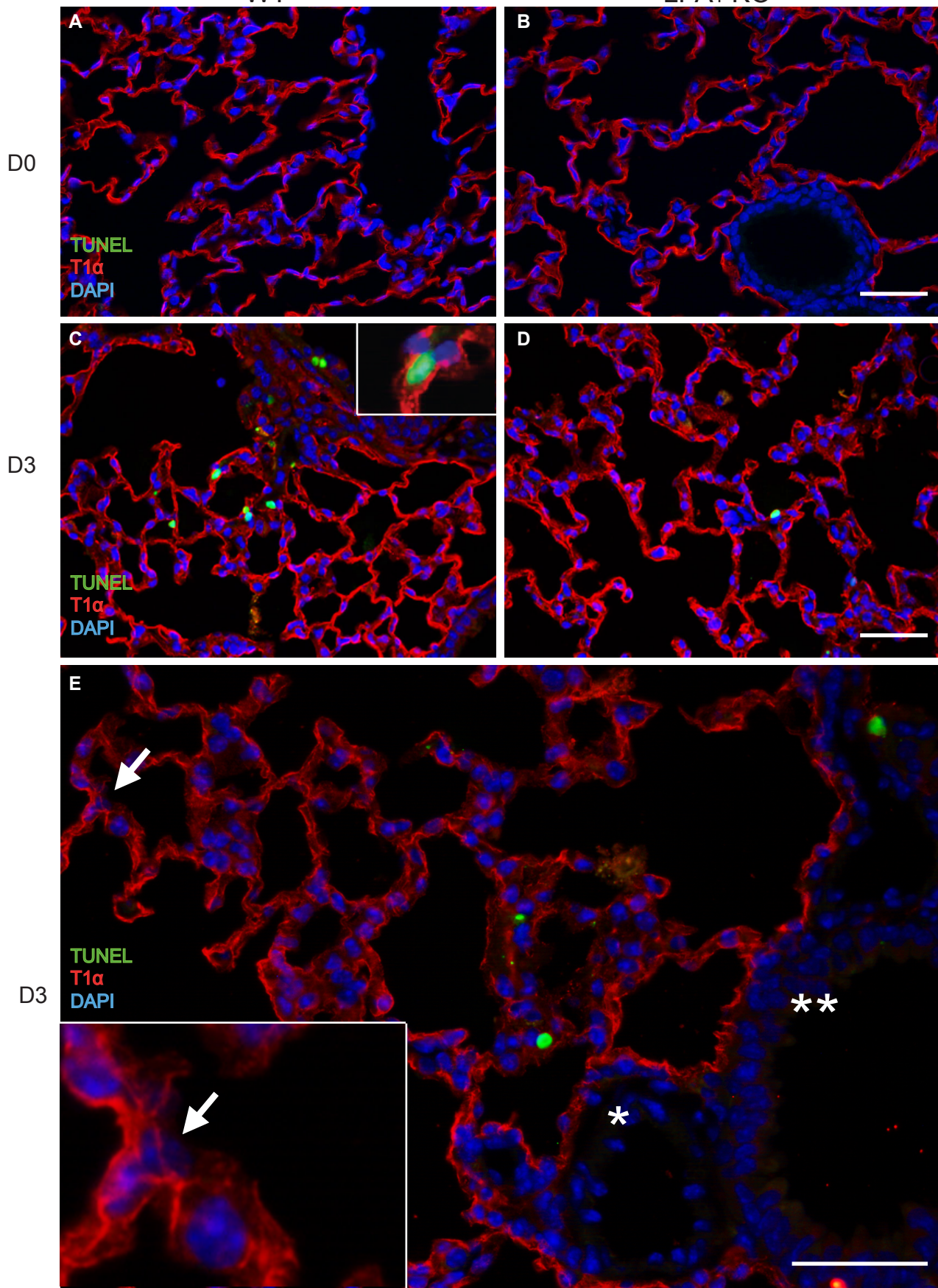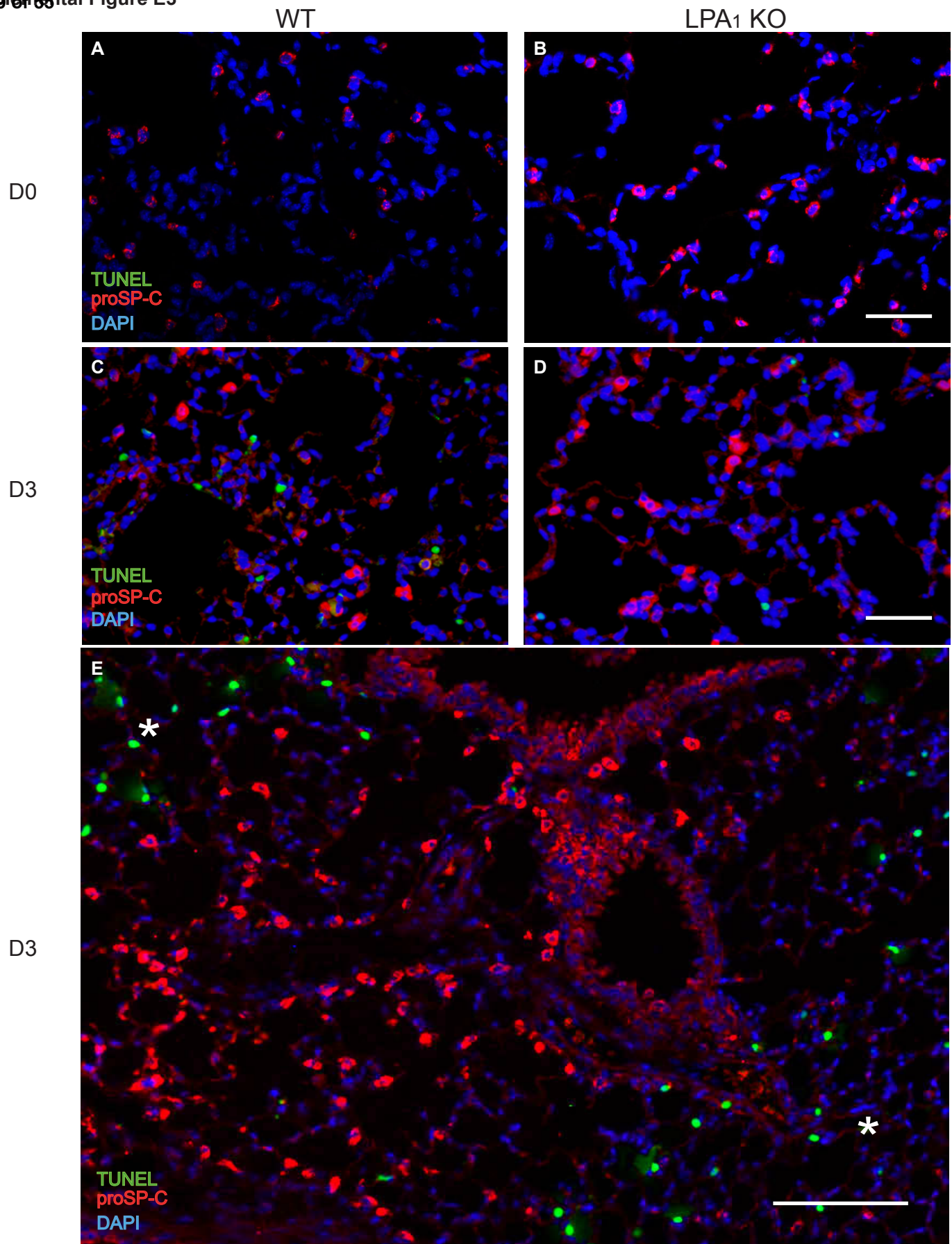
Figure E2. T1α staining for type I alveolar epithelial cells (AECs).
Panel A to E show representative WT and LPA1 KO lung sections with Alexa 555-labeled anti-T1α staining (red) and fluorescein-labeled TUNEL staining (green). Cell nuclei were visualized with DAPI staining (blue). Panel A and B show untreated WT and LPA1 KO lungs. Panel C and D show lungs 3 days post-bleomycin challenge, with fewer TUNEL+ cells in LPA1 KO lung sections. Some TUNEL+ cells were T1α+. Panel E demonstrates the specificity of anti-T1α staining for Type I AECs. The typical T1α labeling of type I AEC surfaces contrasts with the absence of T1α staining of the bronchial epithelium (*) and pulmonary endothelium (**). The main panel white arrowhead indicates a cell with the appearance of a type II AEC that also lacks T1α staining, as shown at higher magnification in the insert panel. Scale bars = 50 μm.

Figure E3. ProSP-C staining for type II alveolar epithelial cells (AECs).
Panel A to E show representative WT and LPA1 KO lung section with Alexa 555-labeled anti-proSP-C staining (red) and fluorescein-labeled TUNEL staining (green). Cell nuclei were visualized with DAPI staining (blue). Panel A and B show untreated WT and LPA1 KO lungs. Panel C and D shows lungs 3 days post-bleomycin challenge, with fewer TUNEL+ cells in LPA1 KO lung sections. Although TUNEL+ cells were not proSP-C+, panel E demonstrates reduced anti-proSP-C staining in areas of lung injury where apoptotic cells are present (*). Scale bars = 50 μm for all images.

Supplemental Figure E4
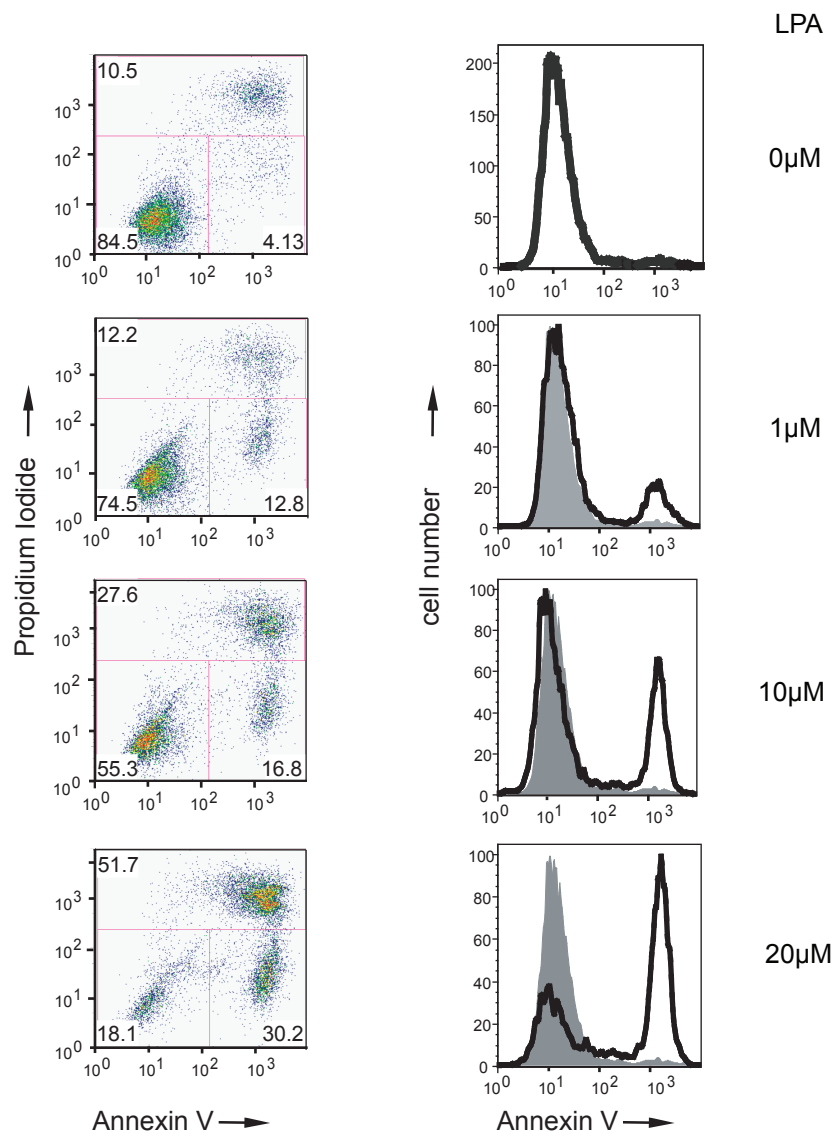
Figure E4. NHBE cell apoptosis induced by LPA was demonstrated by flow cytometry.
LPA dose-dependently induced the apoptosis of NHBE cells grown on low attachment untreated polystyrene.
Apoptotic NHBE cells were identified in these experiments by flow cytometry following staining with annexin V
and propidium iodide (PI), as annexin V-positive, PI-negative cells. These cells are displayed in the lower
right quadrants of the representative dot plots presented (left column). The open black curves in the
corresponding histograms (right column) display the numbers of annexin V-positive and -negative NHBE cells
that were present among the PI-negative populations. The filled grey curves display control cells that were
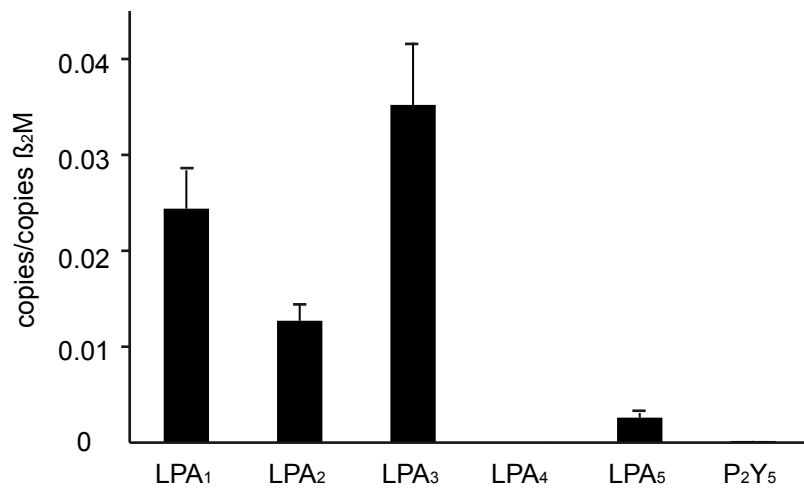not stained with annexin V.

Supplemental Figure E5

Figure E5. NHBE cell LPA receptor expression. Data from one of two independent experiments are presented as mean copies of receptor mRNA relative to copies of β2-microglobulin (β2M) mRNA ± SEM, as determined by quantitative PCR performed on mRNA isolated from n = 3 cultures of NHBE cells in each experiment.

Supplemental Figure E6
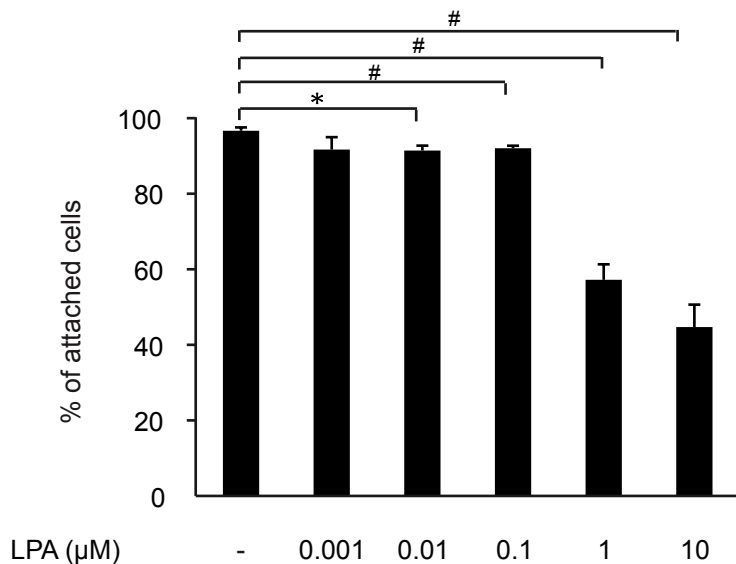
Figure E6. LPA inhibited NHBE cell attachment dose-dependently.
LPA limited the attachment of NHBE cells to high attachment tissue
culture-treated polystyrene in a dose-dependent manner.
Data represent the means of the percentages of attached cells ± SEM;
n = 3 cultures per treatment condition. Attached cells were identified visually
by phase contrast microscopy as having spread, i.e. flattened from their initial rounded
shape such that their nucleii and cytoplasm could be differentiated.
*P < 0.05 and #P < 0.001, LPA-treated vs. untreated NHBE cells, as indicated.
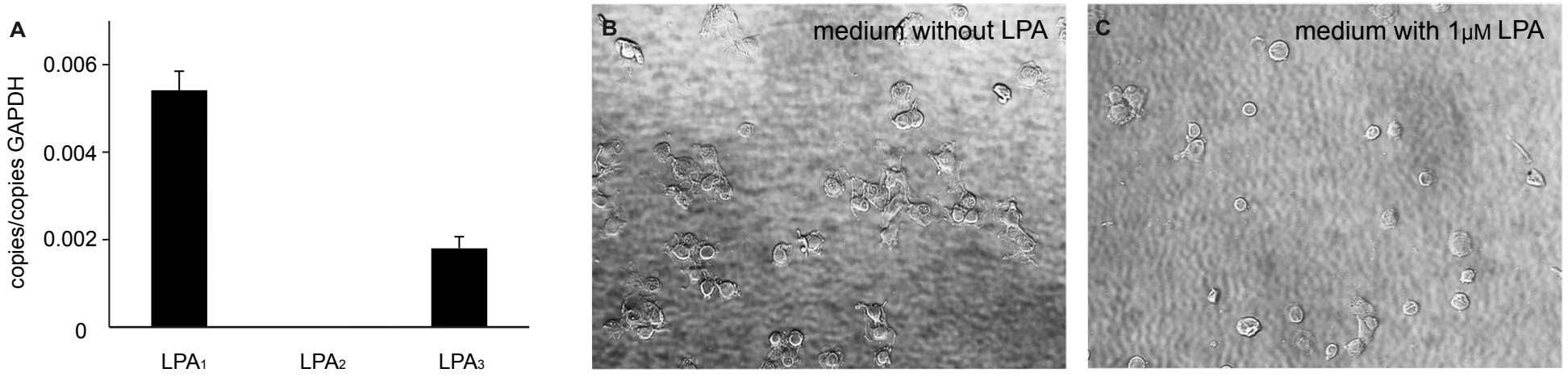
Supplemental Figure E7

Figure E7. R3/1 cell LPA receptor expression and the effect of LPA on R3/1 cell attachment. (A) Mean copies of LPA receptor mRNA relative to copies of glyceraldehyde 3-phosphate dehydrogenase (GAPDH) mRNA ± SEM, as determined by quantitative PCR performed on mRNA isolated from n = 3 cultures of R3/1 cells. (B and C) LPA limited the attachment of rat R3/1 cells to high attachment tissue culture-treated polystyrene. Representative images of the spreading of these cells (B) in the absence of LPA and (C) in the presence of 1μM LPA. Spread cells were identified visually by phase contrast microscopy as having flattened from their **in**itial rounded shape such that the nucleus and cytoplasm could be differentiated.
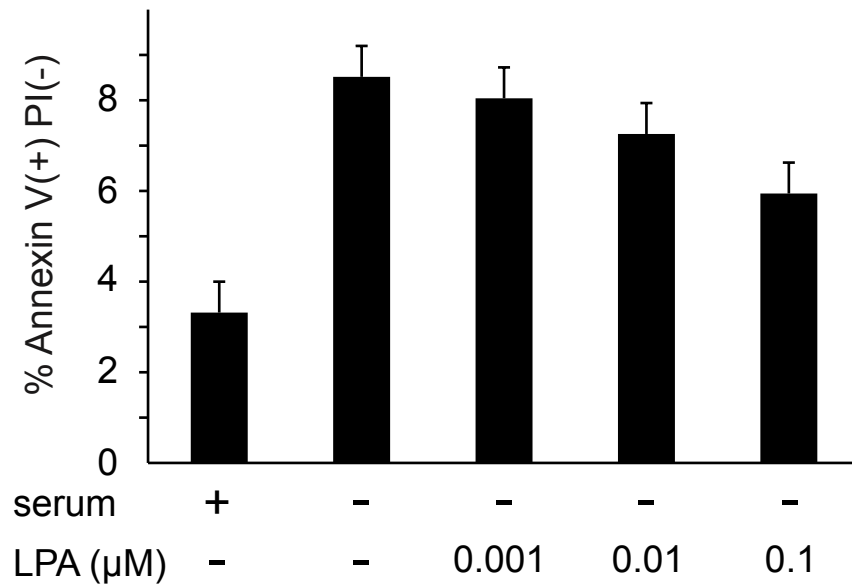
Supplemental Figure E8

Figure E8. Effects of low LPA concentrations on PMLF apoptosis.As presented
in Figure 6A of the manuscript, PMLF apoptosis inducedby serum deprivation for
24 hours was completely prevented by LPA concentrations as low as 1 mM.
Lower LPA concentrations produced trends of reduced PMLF apoptosis when
these cells were grown on high attachment tissue culture-treated polystyrene,
as indicated above, but these trends were non-significant. One-way ANOVA rejected the
hypothesis of equality of the group means, but none of the pairwise comparisons between
untreated PMLF and PMLF treated with these low LPA concentrations were significant
after making Bonferroni post-test corrections.
Apoptotic cells were identified by flow cytometry following staining with annexin V
and propidium iodide (PI), as annexin V-positive, PI-negative cells.
Data represent the means of the percentages of annexin V(+) PI(-) cells ± SEM;
n = 3 cultures per treatment condition.
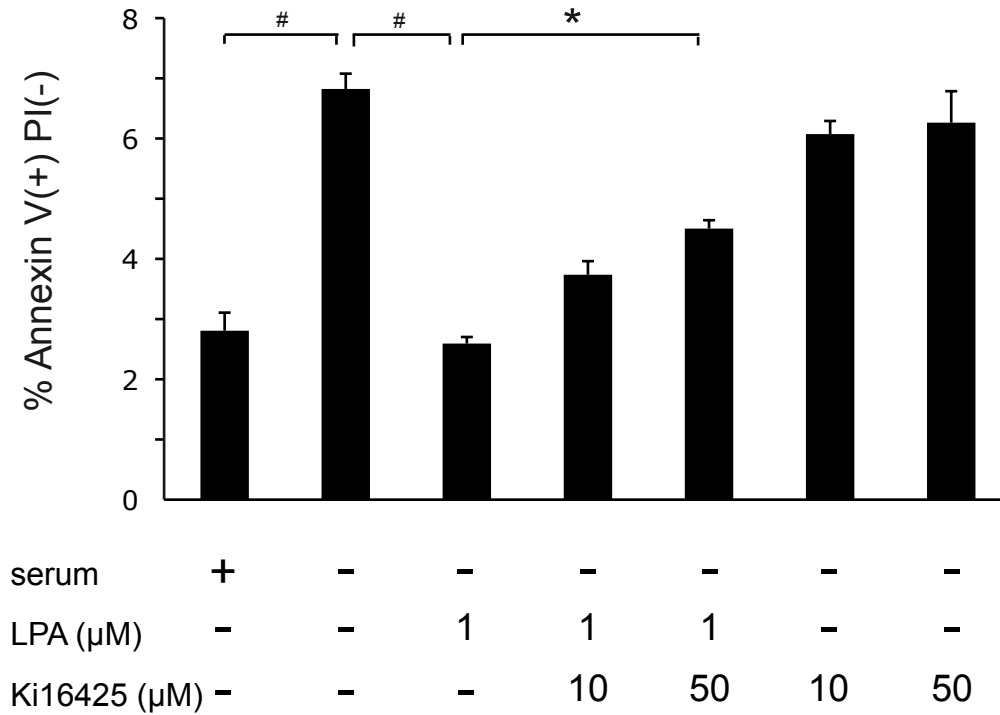
Supplemental Figure E9

Figure E9. Effects of low Ki16245 concentrations on LPA's ability to prevent PMLF apoptosis. As presented in Figure 6B of the manuscript, LPA-induced resistance of PMLF to apoptosis was completely inhibited by 100 mM Ki16425. Lower Ki16425 concentrations partially inhibited LPA's ability to prevent PMLF apoptosis induced by serum deprivation when these cells were grown on high attachment tissue culture-treated polystyrene, as indicated above. #P < 0.001, serum-deprived PMLF vs. PMLF in serum, and serum-deprived PMLF treated with LPA vs. serum-deprived cells not treated with LPA. *P < 0.05, serum-deprived PMLF treated with LPA that were also treated with 50 μM Ki16425 vs. serum-deprived PMLF treated with LPA but not Ki16425. Apoptotic cells were identified by flow cytometry following staining with annexin V and propidium iodide (PI), as annexin V-positive, PI-negative cells. Data represent the means of the percentages of annexin V(+) PI(-) cells ± SEM; n = 3 cultures per treatment condition.